GEOLOGICAL SURVEY OF CANADA
PAPER 90-12

GRAVITY INTERPRETATION ALONG SEISMIC REFRACTION LINES SURVEYED NEAR THE CANADIAN ICE ISLAND DURING 1985

L.W. Sobczak,
J.F. Halpenny, and D.M. Henderson

1991

Energy, Mines and Resources Canada
Énergie, Mines et Ressources Canada

Canada

THE ENERGY OF OUR RESOURCES
THE POWER OF OUR IDEAS

GEOLOGICAL SURVEY OF CANADA
PAPER 90-12

GRAVITY INTERPRETATION ALONG SEISMIC REFRACTION LINES SURVEYED NEAR THE CANADIAN ICE ISLAND DURING 1985

L.W. Sobczak,
J.F. Halpenny, and D.M. Henderson

1991

Available in Canada through
authorized bookstore agents and other bookstores
or by mail from

Canadian Government Publishing Centre
Supply and Services Canada
Ottawa, Canada K1A 0S9

and from

Geological Survey of Canada offices:

601 Booth Street
Ottawa, Canada K1A 0E8

3303-33rd Street N.W.,
Calgary, Alberta T2L 2A7

A deposit copy of this publication is also available for reference
in public libraries across Canada

Cat. No. M44-90/12
ISBN 0-660-13765-8

Price subject to change without notice

Critical Reader

M.J. Drury

Authors' address

L.W. Sobczak
J.F. Halpenny
D.M. Henderson
Geological Survey of Canada
1 Observatory Crescent
Ottawa, Ontario
K1A 0Y3

Original manuscript received: 1990-05-10
Final version approved for publication: 1990-01-20

CONTENTS

GRAVITY INTERPRETATION ALONG SEISMIC REFRACTION LINES SURVEYED NEAR THE CANADIAN ICE ISLAND DURING 1985

Abstract

The structure of the Queen Elizabeth shelf and slope northwest of Axel Heiberg and Ellesmere islands has been analyzed along three profiles. The geophysical and geological information was largely obtained from the Canadian ice island during 1985 as part of the Frontier Geoscience Program. Gravity-density analysis constrained by seismic refraction depths indicate a major sedimentary sequence varying in thickness from 3 to 15 km. The lower portion, consisting of the Sverdrup and Franklinian basins, has in some places been thermally metamorphosed and intruded by mafic rocks. Unmetamorphosed parts of this sequence located over the continental margin have a negative enhanced isostatic gravity signature of anomaly (EIA). These straddle the Sverdrup Rim and extend southward from there to overlie the western Sverdrup Basin within the Queen Elizabeth Islands, where significant deposits of hydrocarbons, largely in the form of natural gas, have been found. Similar hydrocarbon prospects are proposed for the offshore regions associated with negative EIA.

A shallow, high velocity zone detected in a profile normal to the shoreline and interpreted by seismologists as the expression of uplifted faulted blocks, is here interpreted largely as a wall of migrated evaporites which may contain some mafic intrusions of Eurekan age.

Crustal thicknesses vary from 40 km at the shore to 15 km below the Canada Basin.

Résumé

La structure de la plate-forme et du talus continentaux de la Reine-Élizabeth, au nord-ouest des îles Axel Heiberg et d'Ellesmere a été analysée le long de trois profils. Dans le cadre du Programme géoscientifique des régions pionnières, on a recueilli au cours de 1985, surtout à partir de l'île de glace canadienne, des données géophysiques et géologiques. Une analyse de la pesanteur et de la densité, étayée de profondeurs de sismique réfraction, indique une importante séquence sédimentaire dont l'épaisseur varie de 3 à 15 km. La partie inférieure, composée du bassin Sverdrup et du bassin Franklin, a été, par endroits, métamorphisée thermiquement et recoupée de roches mafiques. Les parties non métamorphisées de cette séquence, situées au-dessus de la marge continentale, présentent une signature gravimétrique négative des anomalies isostatiques améliorées. Elles chevauchent la bordure de Sverdrup et s'étendent vers le sud recouvrant la partie occidentale du bassin Sverdrup au sein des îles de la Reine-Élizabeth où l'on a découvert des gisements importants d'hydrocarbures, en général sous la forme de gaz naturel. La présence de zones d'intérêt d'hydrocarbures semblables est proposée pour les régions extracôtières associées à des anomalies isostatiques améliorées négatives.

Une zone peu profonde à vitesse élevée, décelée dans un profil perpendiculaire au littoral et considérée par les sismologues comme l'expression de blocs faillés soulevés, est ici surtout interprété comme un mur d'évaporites ayant migré et pouvant contenir quelques intrusions mafiques d'âge eurékien.

L'épaisseur de la croûte varie de 40 km au rivage à 15 km au-dessous du bassin Canada.

INTRODUCTION

This study is part of the Frontier Geoscience Program of the Geological Survey of Canada, which started in 1984. The purpose of the program is to investigate the Canadian polar margin with a major effort being conducted from a Polar Continental Shelf Project base camp on a Canadian ice island named "Hobson's Choice", off the coast of Axel Heiberg Island. During April, 1985, and from April to May, 1986, 140 gravity and 124 water depth measurements were made along seismic refraction lines (Asudeh et al., 1989). Field procedures and instrumentation have been discussed by Sobczak and Schmidt (1985); Sobczak and Weber (1986); Weber and Sobczak (1986); and Sobczak and Weber (1987). In 1987, nearly 2000 gravity and water depth measurements were made in the area west and northwest of Axel Heiberg Island, over the Queen Elizabeth shelf and slope and north-eastern end of the Canada Basin adjacent to the Alpha Ridge in order to fill in a void in gravity coverage in an area northwest of Axel Heiberg Island. (Weber and Cooper, 1988). Gravity observations have also been made over the unmapped areas of Axel Heiberg and Ellesmere islands (Fig. 1) but these observations were not available at the time of preparation of this report.

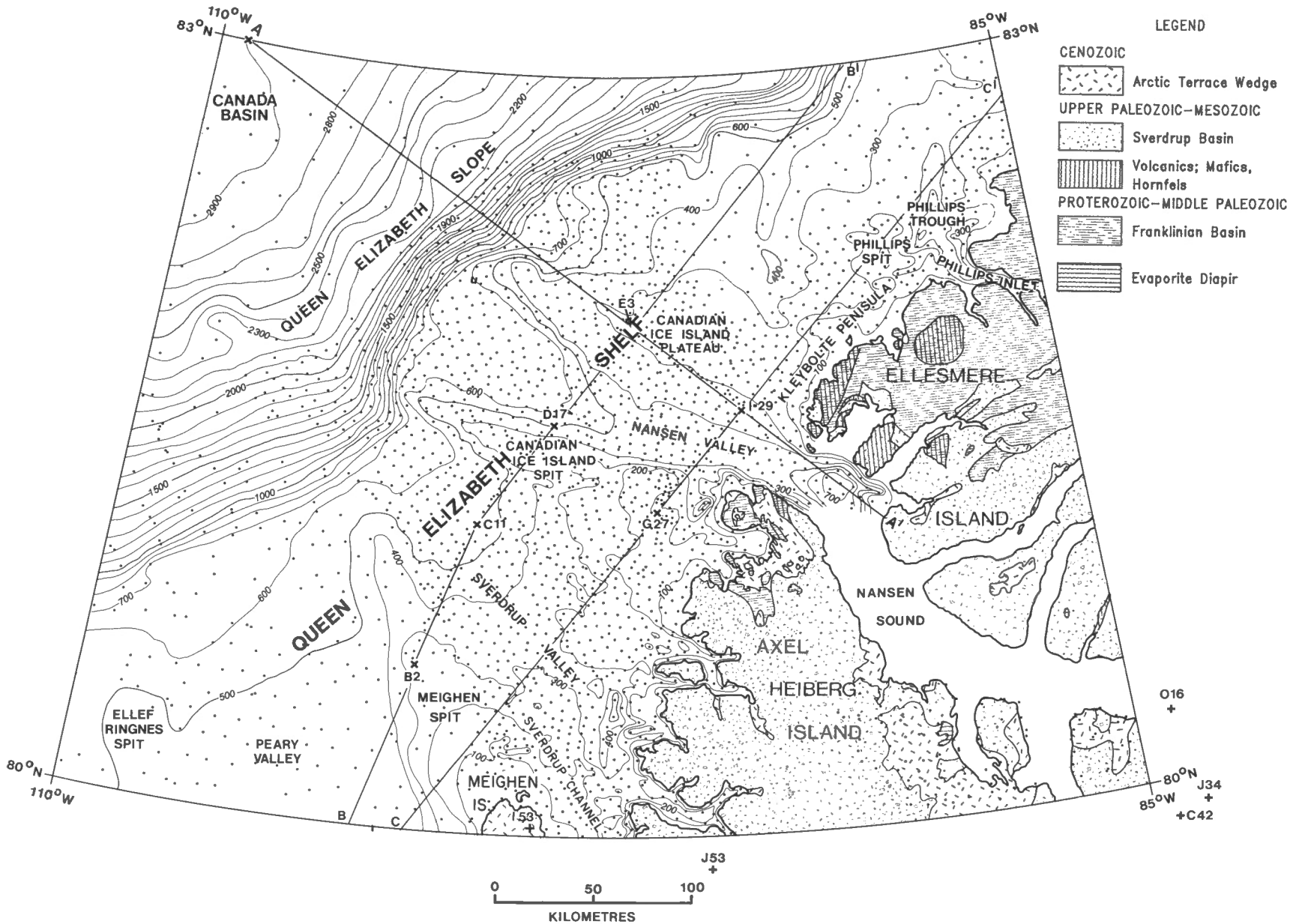

Figure 1. Location map showing bathymetry offshore contoured at 100 m water depth intervals, geology onshore, profiles, and locations of water depth and gravity measurements shown by dots. Drill holes are shown by crosses, a letter and a number. Seismic refraction shot points are shown by letter followed by a number. Profile locations of gravity analysis, including the seismic refraction lines, are also indicated. The geology shown in Figure 1 was taken from geological maps 1305A, 1309A, 1310A, and 1311A compiled by Thorsteinson and Trettin (1971a,b,c,d).

Gravity and bathymetry over the Arctic prior to 1985 have been discussed by Sobczak (1978); Sobczak and Sweeney (1978); and Sobczak et al. (1990). Sobczak et al. (1990) compiled a gravity anomaly map of the whole Arctic region north of 64°N latitude at a scale of 1:6 000 000 depicting Bouguer anomalies on land and free-air anomalies offshore. Free-air (FA), Bouguer (BA), isostatic (IA) and an enhanced isostatic gravity anomaly (EIA) maps for the Arctic have been prepared and discussed by Sobczak and Halpenny (1990a,b). The IA and EIA were developed in order to minimize distortions and masking effects due to: large density boundaries such as between water and sediments and between crust and mantle along a continental margin; isostatic effects due to some form of compensation resulting from loads on the crust; regional relationships between isostatic anomalies and water depth or elevation caused probably by thermal and glacial effects at the crust-mantle boundary. The EIA map is considered the best for outlining anomalies related directly to geological structures, in a region where topography (and bathymetry) is variable and where oceanic, transitional and continental crusts are present.

Bathymetry, geology, location of seismic refraction lines surveyed in 1985 and modelled and published (Asudeh et al., 1989) and location of drill holes used for velocity, density and lithological control, shown in Figure 1, are superimposed on the EIA map (Fig. 3) for easy reference. Age, formation, lithology, density and interval velocities for seven drill holes (Fig. 4) were obtained from files at the Canada Oil and Gas Lands Administration of the Department of Indian and Northern Development at Ottawa. Additional drill hole information was obtained from Sobczak and Overton (1984) and from Sobczak et al. (1970). The purpose of this report is to determine the geological structure below the continental margin using both the seismic refraction model and gravity as constraints. This structure can be extended in plan using the EIA map. Aeromagnetic data were compiled using data from the Geological Survey of Canada (GSC) which covered the southern part of the map (south of the seismic refraction line E_3-I_{29}) and from the National Geophysical Data Centre (NGDC), Boulder Colorado which covered the northern part. These data were compiled by McGrath and Fraser (1987) for the Magnetic Anomaly Map of Arctic Canada.

GEOLOGY

The study area is located on the Queen Elizabeth Shelf, which forms the northern part of the continental crust of northern Canada offshore from the Queen Elizabeth Islands (QEI). The QEI consist of Precambrian gneissic crystalline basement covered by Phanerozoic sediments. This basement outcrops on the southeastern end of Ellesmere Island and is covered to the northwest by a succession of overlapping basins that have progressively migrated northward. In a few places, basement is overlain by Proterozoic sandstone and carbonates but it is generally overlain by Cambrian carbonates which form the lowest part of a sequence of carbonates, clastic and evaporite rocks of Cambrian to Devonian age of the Franklinian Basin. The southern part of this basin (the Arctic Platform) is undeformed but the northern part, forming the Franklinian shelf and trough, was deformed during the Ellesmerian Orogeny of late Devonian and Mississippian age. These deformed rocks outcrop along two northeast-southwest belts; one runs from northern Greenland to eastern, central, and southern Ellesmere Island and the other along the northern part of Ellesmere Island as noted in Figure 1.

After the Ellesmerian Orogeny, the Sverdrup Basin sequence formed on the deformed part of the Franklinian Basin. The basin was filled with evaporites and terrigenous clastics derived mainly from the south and east between Carboniferous and Cretaceous times. Volcanic episodes took place during Permian and Cretaceous times. The Cretaceous event is the most significant, with extensive mafic intrusions and volcanism along the northern (Fig. 1) (Embry and Osadetz, 1988) and southern flanks of the eastern half of the basin. These mafic rocks are dated from 110 to 88 Ma: on northern Ellef Ringnes Island 110 to 102 Ma (Larochelle et al., 1965), on Axel Heiberg Island 95 to 88 Ma (Ricketts et al., 1985) and on Ellesmere Island 93 to 88 Ma (Trettin and Parrish, 1987). Sedimentation in the Sverdrup Basin ended by the Eurekan Orogeny which acted between the Late Cretaceous and mid Tertiary time. During this time regional uplift of the Sverdrup Rim took place which affected the northern part of Axel Heiberg and Ellesmere islands. During Maastrichtian time (about 67 Ma) the uplifted segment of the Sverdrup Rim started to collapse to the southeast while the Eurekan Orogeny continued to produce uplift and erosion in Ellesmere Island. This was followed by broad folding, reverse faulting and thrusting in response to northwest-southeast directed crustal compression that produced at least 60 km of crustal shortening in the eastern QEI during 45 to 30 Ma ago (Ricketts and McIntyre, 1986).

Clastic detritus produced by the Eurekan tectonism migrated mainly northwestward to form the Arctic Terrace Wedge which is a part of the Canadian Arctic Margin Basin (Sobczak et al., 1986) that covers the present continent-ocean boundary. These Cenozoic sediments thicken seaward to at least 4.5 km as discussed herein and possibly to 10 km northwest of Ellef Ringnes Island (Sobczak et al., 1986).

To summarize, northern Axel Heiberg and northwestern Ellesmere islands (Fig. 1) show the Arctic Terrace Wedge in part overlying Sverdrup and Franklinian basin rocks which are greatly metamorphosed, overlain and intruded by mafics in this area. This zone of volcanism (Embry and Osadetz, 1988) is extended offshore using gravity and seismic refraction analysis along lines done in 1985 by Asudeh et al. (1989).

RESULTS

Bathymetry

Locations where water depths and gravity measurements were taken since 1960 are shown by dots (Fig. 1). The water depths are contoured at 100 m intervals. Generally the Canadian polar margin is much narrower than the margin off the USSR and the Scandinavian countries (Johnson et al., 1979 and Perry et al., 1986). It has a shelf-slope break considerably deeper than for the wider shelves of the Arctic Ocean and the world average (about 200 m, Worzel, 1968).

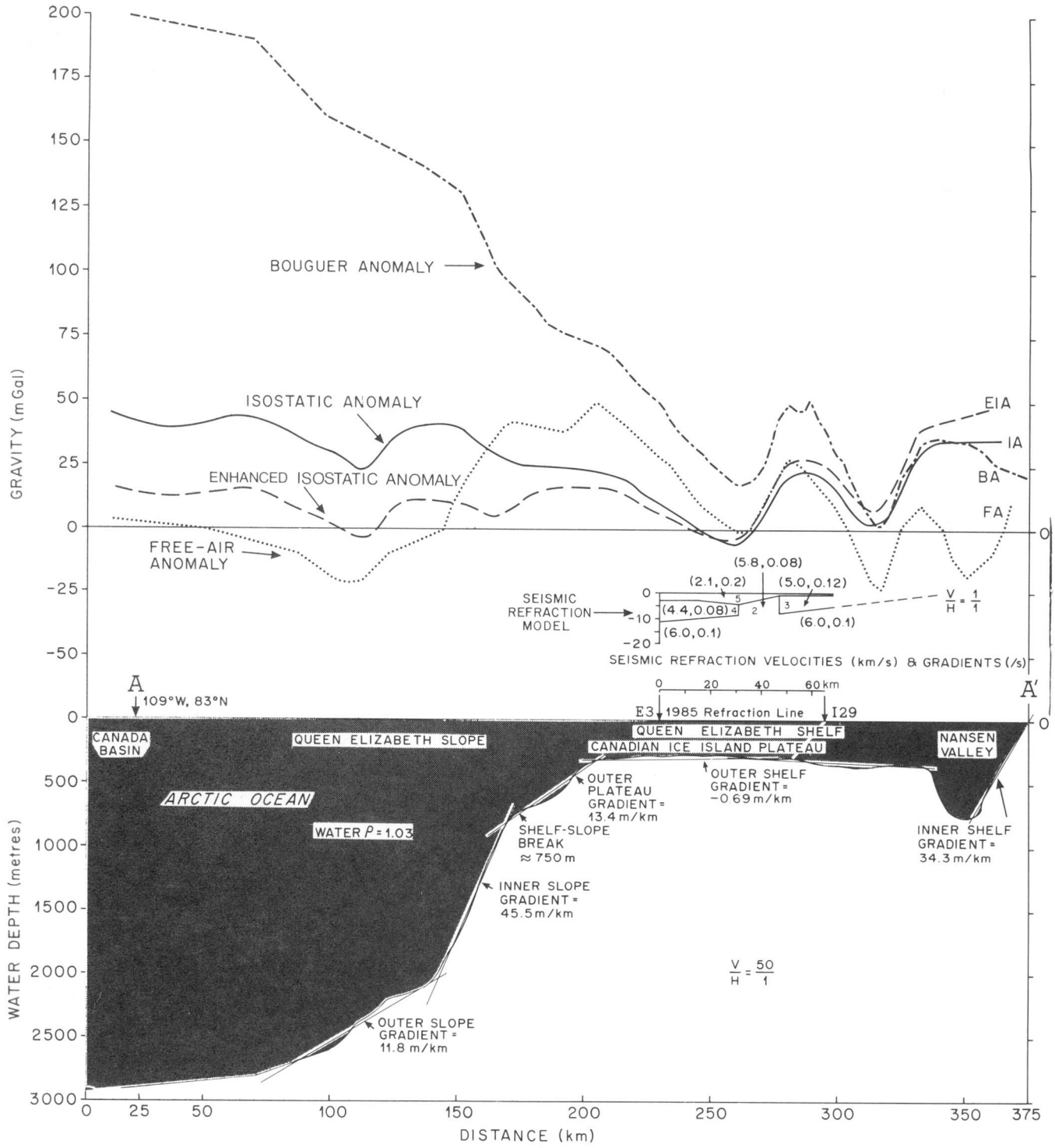

Figure 2. Profile A-A′ across the Canadian polar margin showing bathymetry, free-air, Bouguer, isostatic and enhanced isostatic anomalies and the seismic refraction model between E_3-I_{29}.

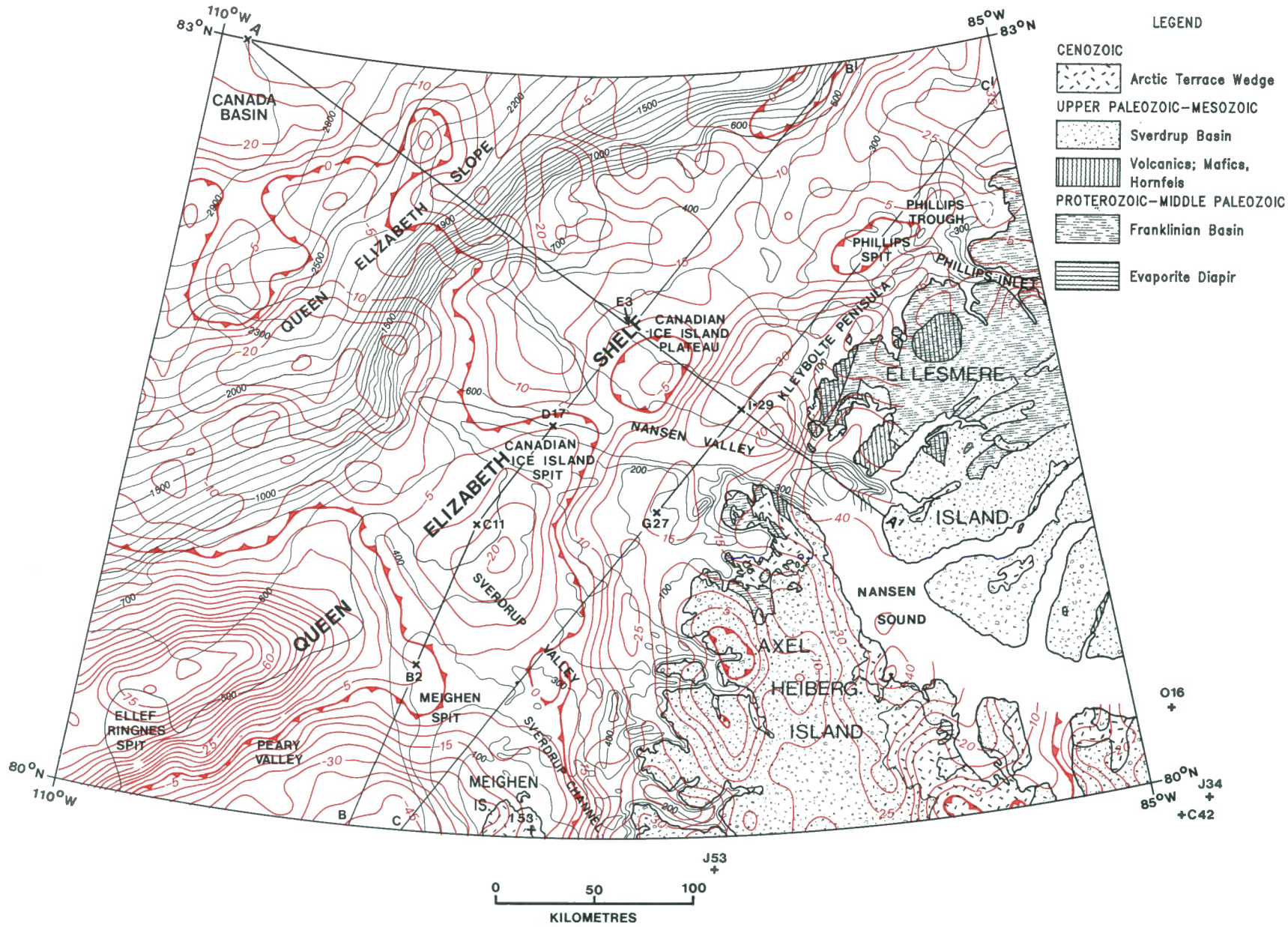

Figure 3. Enhanced isostatic anomalies are shown in red at contours at 5 mGal intervals. Zero anomaly contours are heavier with barbs on the negative anomaly side.

The depth to the shelf-slope break in the Canadian sector increases from 100 to 200 m north of the Mackenzie Delta, to 500 m off Banks Island, to 650 m northwest of Ellef Ringnes Island, to 750 m northwest of Axel Heiberg Island and decreases again to about 500 m north of Ellesmere Island (Sobczak et al. 1986). The area under investigation lies in the region with the greatest amount of submergence and the most pronounced northwest-southeast trending irregular morphology. The valleys and ridges on the continental shelf appear to be seaward extensions of features observed along the Queen Elizabeth Islands. For example, going from northeast to southwest along the shelf, the Canadian Ice Island Plateau lies off Kleybolte Peninsula of northwestern Ellesmere Island; Nansen Valley is the seaward extension of Nansen Sound; Canadian Ice Island Spit extends from northern Axel Heiberg Island; Sverdrup Valley extends from Sverdrup Channel; and Meighen Spit extends from Meighen Island.

These features may be related to broad northwest-southeast folding that took place in the eastern Queen Elizabeth Islands during the end of the Eurekan Orogeny and may also be the result of the crustal shortening proposed by Ricketts and McIntyre (1986). The valleys become deeper and narrower from the southwest to the northeast, probably indicating more severe tectonism towards the northeast; this feature is unlikely to be caused by glaciation effects. However, glaciation as discussed by Pelletier (1964) probably emphasized these tectonic features.

The various bathymetric characteristics normal to the continental margin are best demonstrated by Profile A-A′ (Fig. 2). This profile shows a very steep (34 m/km) inner shelf gradient with a deep (700 m) trough at the mouth of Nansen Sound followed by a relatively flat shelf. The outer platform has a gradient of about 13 m/km, some two and half times steeper than off northwest of Ellef Ringnes Island (Sobczak et al., 1986).

Free-air anomalies

Over the continental shelf, generally, free-air anomaly highs overlie the shelf-slope break, plateaus and spits and lows overlie the valleys but not always in a one to one relationship. For example, along seismic line E_3 -I_{29} (Fig. 2) where the bathymetry is more or less at a uniform depth of about 300 m the free-air anomalies vary from -3 mGal to 27 mGal indicating intra-crustal density variations. If these anomalies, in other places, are influenced by water depth variations the limits of the anomalous gravity becomes difficult to estimate on a free-air anomaly map.

Bouguer anomalies

Bouguer anomalies over water incorporate a correction for the mass deficiency of the water layer and remove the gravity variations associated with an irregular bottom morphology. However, going seaward, as the bathymetry gets deeper the gravity anomalies become larger, in excess of 210 mGal. These large values tend to obscure smaller anomalies. Gravity anomalies which get progressively lower towards higher terrain or progressively higher towards deeper water are largely the effect of isostatic compensation. These topographic correlations for both free-air and Bouguer anomalies for the whole Arctic region north of 64°N latitude have been discussed by Sobczak and Halpenny (1990a,b). These gravity-topographic correlations are linear over certain height or depth intervals and affect the utility of using free-air and Bouguer anomalies for geological interpretation. These effects were minimized by using isostatic corrections.

Isostatic anomalies

Isostatic anomalies were developed on a continental basis with large data sets by methods outlined by Simpson et al. (1986a,b) and by Goodacre et al. (1987). Both methods utilize isostatic compensation as defined by Airy (1855): crustal loads are compensated at depth by roots and anti-roots in much the same way as an iceberg floating in water. The compensating masses are placed at an equilibrium depth of 30 km. The gravity effect of these masses are computed by methods outlined by Goodacre et al. (1987); Sobczak and Halpenny (1990a,b). These total isostatic corrections are removed from the Bouguer anomalies to produce isostatic anomalies (IA). Many of the problems associated with topography, edge effects and isostatic effects are largely removed in this type of anomaly map. However, in a study of the whole Arctic region north of 64°N latitude, comparisons of isostatic anomalies with elevation or water depth indicated that linear correlations with topography still existed (Sobczak and Halpenny 1990a,b). These correlations were removed from the isostatic anomaly map to produce an enhanced isostatic anomaly map which is used in the interpretation of the gravity along the seismic refraction lines.

Enhanced isostatic anomalies

An enhanced isostatic anomaly (EIA) map is shown in Figure 3. This map removes relationships between anomalies and topography; topography, edge, boundary, isostatic and regional gravity effects have been minimized. The zero anomaly contour generally delineates the edges of anomalous masses within the crust.

EIA anomalies, varying from a high of + 80 mGal to a low of -45 mGal, outline a geologically complex area of the margin and mainland. The most pronounced anomaly (80 mGal) is the positive one over the shelf-slope break northwest of Ellef Ringnes Island, which has been explained by Sobczak (1975a,b), Sobczak et al. (1986), and Sweeney et al. (in press) as being the effect of an uncompensated load of recent sediments at the shelf-slope break. However, unlike the free-air anomalies shown by Sobczak and Halpenny (1990b) which give the impression that they (magnitudes 50 to 60 mGal) extend to the Axel Heiberg and Ellesmere island shelf edge (Weber, 1986), the EIA map (Fig. 3) shows no such extension of positive anomalies.

Surrounding this high is a region of extensive lows overlying the Queen Elizabeth slope and shelf. The seismic refraction line B_2-D_{17} bisects this region of gravity lows and touches the eastern end of the large gravity high (80 mGal). This line will be discussed later. East of the lows the area is

generally covered by positive anomalies, which on land relate to the thinning of Franklinian and Sverdrup Basin rocks and the existence of mafic rocks (Fig. 1). Seismic refraction lines G_{27}-I_{29} and E_3-I_{29} are located in this positive region and provide control sections for the analysis of the gravity data.

INTERPRETATION

Geological control on land was provided by surface geology (Thorsteinsson and Trettin, 1971a,b,c,d) and drill hole data from Meighen Island (I53), Axel Heiberg Island (J53), Amund Ringnes Island (H40, M05) and Ellesmere Island (O16, J34, C42) and offshore by seismic refraction data along lines E_3-I_{29}, G_{27}-I_{29} and B_2-C_{11}-D_{17} (Asudeh et al., 1989). The drill hole data from west to east are taken from an area of gravity lows (Meighen Island area), an area of gravity highs (Axel Heiberg and Amund Ringnes islands), and to an area of gravity lows (Ellesmere Island).

Drill hole data

In general, the lithology of Cenozoic and Mesozoic rocks varies between argillaceous and arenaceous, whereas the Paleozoic rocks contain a much greater abundance of carbonate. In places these rocks are intruded by varying amounts of igneous mafic rocks. Although lithology partially affects the densities, they appear to have a stronger correlation with age, which in turn may be related to maximum depth of burial (Sobczak et al., 1970; Sobczak and Overton, 1984; Sobczak et al., 1986). Comparisons are made between densities and age. In general interval velocities appear to be a function primarily of current depth and degree of metamorphism. However, in detail, lithology does have a local (about one metre of depth interval of drillhole) effect but this is of no consequence to the means determined over longer density and seismic velocity intervals (about 100 m) that have remained generally constant. These parameters are discussed separately in order to provide constraints for the gravity-density and seismic velocity models.

Densities

Bulk densities are taken from compensated neutron formation density logs. Average densities are estimated by visual inspection over intervals, of about 100 m, where density levels are more or less constant while ignoring the local spiky characteristic of the densities. Mean densities for these various levels are then weighted according to thickness to obtain the mean density for a particular age (Period) interval. These mean values are shown in Figure 4.

Densities from drill holes H-40, M-05 and J-53 for a particular period for Amund Ringnes and Axel Heiberg islands are much higher than for corresponding periods in other drill holes on Ellesmere Island. This increase in density is probably due to thermal metamorphism of the sedimentary rocks initiated when they were heavily intruded by mafic igneous rocks up to the base of the Kanguk Formation of Early Cretaceous age (about 75 Ma ago). In addition, these mafic rocks are quite dense (varying from mean values of 2.83 to 2.99 Mg/m^3, Fig. 4) and represent a significant portion of the drill hole column (from 23 to 27%, Fig. 4).

An estimate of the effect of metamorphism on the density of sediments was made by comparing mean densities of sedimentary rocks for periods within and outside the zone of volcanism (Embry and Osadetz, 1988) associated with intrusion of the mafic igneous rocks. Table 1 shows mean densities from various drill holes taken from Sobczak and Overton (1984) and from Figure 4. These mean density values from Table 1 were plotted in Figure 5 from west to east; the western region is largely unmetamorphosed and the eastern region is metamorphosed as outlined by the positive enhanced isostatic anomalies shown in Figure 3. All the Cretaceous, Jurassic and Triassic periods show an increase in density of the sediments varying from 0.15 to 0.19 Mg/m^3 for a mean increase of 0.17 Mg/m^3 towards the zone of volcanism on Axel Heiberg and Ellesmere islands (Embry and Osadetz, 1988). The mean density for mafic igneous rocks weighted according to their thickness from six holes is 2.91 Mg/m^3 (drill hole 068 has a mean density for mafic rocks of 2.90 Mg/m^3; N06, 2.87; L41, 2.95; H40, 2.90; J53, 2.83; and C42, 2.99).

Model densities

Model densities were determined for three sedimentary successions; (1) the Canadian Arctic Margin Basin — Arctic Terrace Wedge; (2) Sverdrup Basin, and (3) Franklinian Basin.

These successions appear to be the geological intervals recognized in the seismic refraction models which are used for control of the gravity-density models.

The Canadian Arctic Margin Basin (Arctic Terrace Wedge) consists of mainly arenaceous Tertiary and argillaceous Late Cretaceous sediments as indicated by drill hole I-53 on Meighen Island. An average density of 2.21 Mg/m^3 obtained over a 2.5 km thick interval for the arenaceous portion is taken to be representative of this sequence. The lower portion is more dense (2.45 Mg/m^3), and the upper portion is less dense (2.04 Mg/m^3 obtained from drill hole K-28 on the north side of Ellef Ringnes Island, Sobczak and Overton, 1984).

The mean density of the Mesozoic and Upper Paleozoic rocks of the Sverdrup Basin is determined for unmetamorphosed and thermally metamorphosed rocks as indicated in Table I and shown in Figure 5. If we assume Cretaceous, Jurassic and Triassic with upper Paleozoic rocks to have equal thicknesses with corresponding mean densities of 2.25, 2.36 and 2.47 Mg/m^3 for unmetamorphosed rocks, then an average density of 2.36 Mg/m^3 is determined. However, a north-south structural section (Sobczak et al., 1986) across the Sverdrup Basin reveals a slightly different ratio of thicknesses based on thickness of sediments in the middle of the basin; Cretaceous = 2.8 km, Jurassic = 1.4 km and Triassic with upper Paleozoic = 3.9 km. By using these ratios the mean value is adjusted from 2.36 to 2.37 Mg/m^3 and is used in this analysis. The mean density could even be slightly higher

Table 1. Mean Densities (Mg/m3) for Period intervals and the Number of Drill Holes used for this Mean Value

	J60, B64, D68, D73 Melville Is.	C15 Lougheed Is.	023, N06 King Christian Is.	L50, H37, L4 Ellef Ringnes Is.	153 Meighen Is.	144, H40, MO5 Amund Ringnes Is.	J53 Axel Heiberg Is.	C42, 016, J34 Ellesmere Is.
Tertiary	---	---	---	---	2.21/1	---	---	2.50/2
Cretaceous	2.20/3	2.25/1	---	2.32/2	2.45/1	---	---	2.40/3
Jurassic	2.34/4	2.43/1	2.23/1	2.43/2	---	2.56/2	2.68/1	2.49/3
Triassic	2.39/3	2.51/1	2.54/2	2.48/2	---	2.70/1	2.67/1	2.55/2
Permian	2.54/3	---	---	---	---	---	---	2.67/1

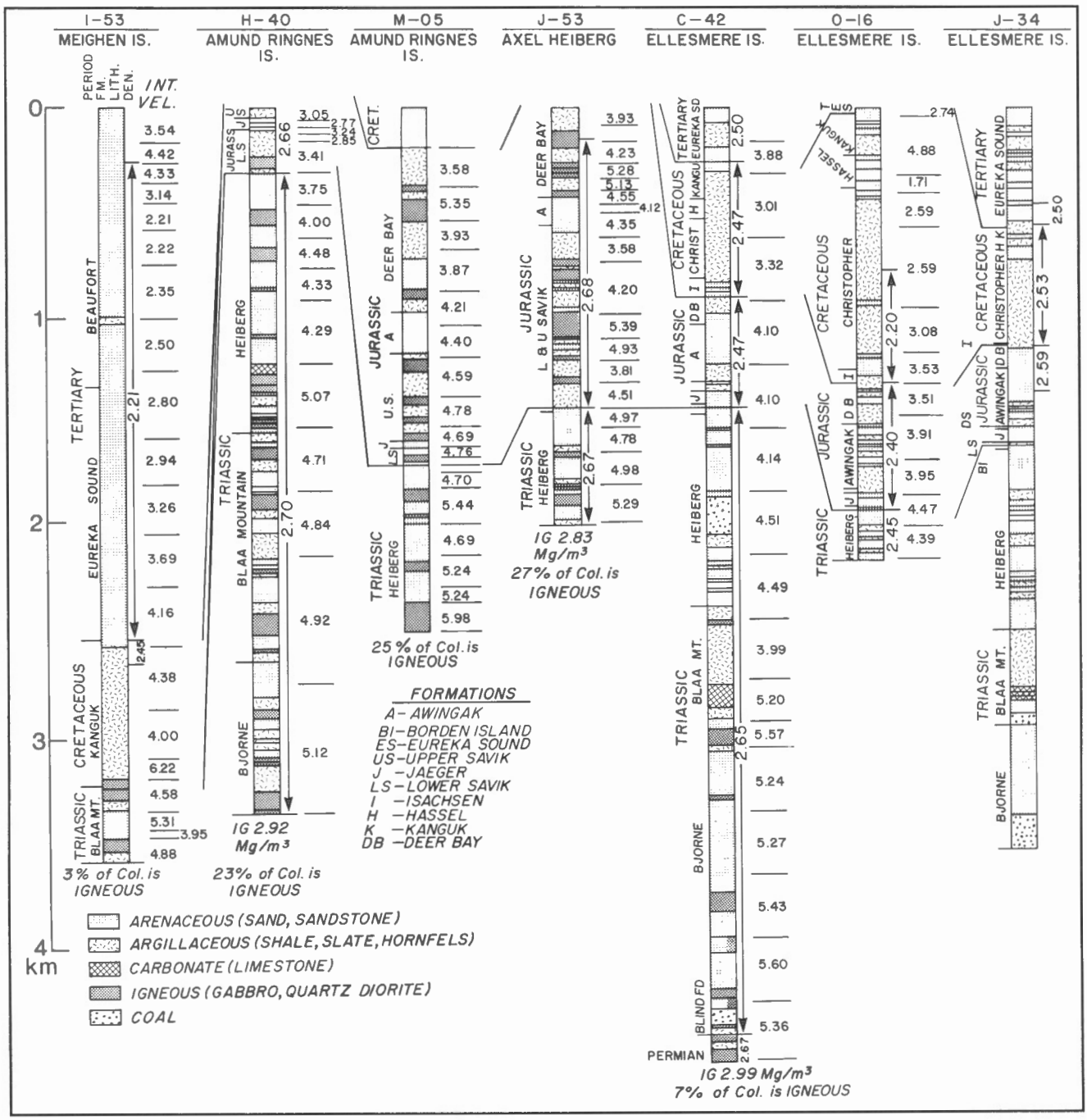

Figure 4. Lithology, age, formation, depth, well number location, averaged compensated formation densities (DEN, Mg/m^3), and internal adjusted sonic velocities for the most northerly drill holes located in Figure 1. Ig = igneous rocks.

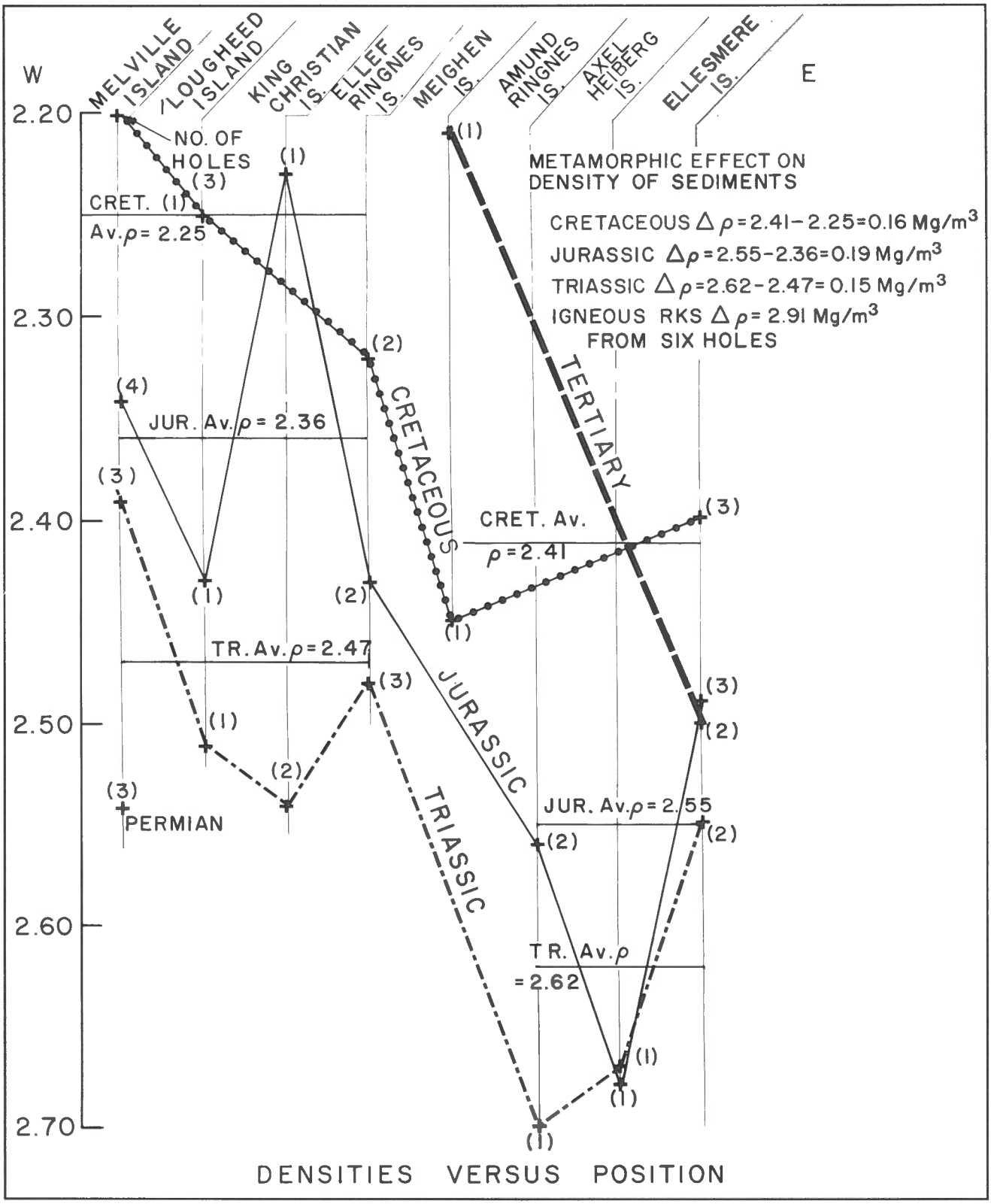

Figure 5. Averaged densities (Mg/m^3) from different drill holes shown in Table 1 according to geological periods, from Melville Island in the western Queen Elizabeth Islands to Ellesmere Island in the east.

Table 2. Densities used in Model Analysis for Unmetamorphosed, Metamorphosed and Intruded with Mafic Rocks

Major Tectonic Units	Mean Density Mg/m³	Density Contrast Mg/m³	Mean Density Mg/m³	Density Contrast Mg/m³	Mean Density Mg/m³	Density Contrast Mg/m³
	Unmetamorphosed		Metamorphosed		Intruded with Mafics	
Canadian Arctic Margin Basin (Arctic Terrace Wedge)	2.21	-0.54	---	---	---	---
Sverdrup Basin	2.37	-0.38	2.54	-0.21	2.64	-0.11
Franklinian Basin	2.66	-0.09	2.75	0.00	2.79	+0.04
North American Craton	2.75	0.0	2.75	0.00	2.79	+0.04

Table 3. Adjusted Sonic Log Velocities

Type Region	Drill Hole Number	Above Mid-Triassic Velocity km/s	Above Mid-Triassic Velocity Gradient /s	Below Mid-Triassic Velocity km/s	Below Mid-Triassic Velocity Gradient /s
Metamorphosed	H-40	3.81	2.21	4.58	0.18
	M-05	3.77	0.93		
	J-53	3.88	0.93		
		-----	-----		
	Average	3.82	1.36		
Unmetamorphosed	I-53	2.18	1.05		
	O-16	2.59	1.36		
	C-42	3.30	0.83	4.72	0.22
		-----	-----		
	Average	2.69	1.08		

(2.42 Mg/m^3) if the individual formations are taken into account as indicated by Sobczak et al. (1986), but this detail was not warranted in this study. Metamorphism of the Sverdrup Basin rocks could also increase the average density by 0.17 Mg/m^3 from 2.37 to 2.54 Mg/m^3 as discussed earlier. If igneous mafic rocks are included in the column (could represent up to 27%, J-53, Fig. 4) then the average density could increase again by 0.10 Mg/m^3.

The Franklinian Basin mean density determination is a little more ambiguous due to a lack of drill holes within these rocks locally and must rely on results determined a considerable distance from this survey area (Sobczak et al., 1986). However, by using Sobczak et al.'s (1986) density values, and assuming equal amounts of carbonates (2.75 Mg/m^3), arenaceous (2.60 Mg/m^3) and argillaceous (2.64 Mg/m^3) rocks, a mean density of 2.66 Mg/m^3 is obtained. If these rocks were metamorphosed due to compaction or heating then an average density of 2.75 Mg/m^3 may be obtained. If igneous mafic rocks are included then the mean density increases by 0.04 Mg/m^3.

Evaporites containing impurities in the Sverdrup and Franklinian basins were taken to have a mean density of 2.31 Mg/m^3 (Sobczak et al., 1986). This value was used as a constraint in the models of this paper.

The Archean crystalline basement (mainly granitic gneiss) of the North American Craton, taken as a standard crust, has a mean density of 2.75 Mg/m^3 at the surface (Sobczak et al., 1970) increasing to a density of 3.00 Mg/m^3 at the base of the crust (Sobczak et al., 1986).

The upper mantle was determined to have a density of 3.40 Mg/m^3 with a density contrast of 0.4 Mg/m^3 between upper mantle and lower crustal rocks at levels deeper than 20 km, but the contrast may be less than 0.25 Mg/m^3 at shallower levels such as below the deep ocean (Sobczak et al., 1986).

Summaries of densities and density contrasts for unmetamorphosed, metamorphosed and mafic intruded rocks are shown in Table 2. These density contrasts were used in the gravity-density models. For example density and density contrasts for the Sverdrup Basin rocks are shown when they are unmetamorphosed (2.37 - 2.75 = -0.38 Mg/m^3), metamorphosed [(2.37 + 0.17) - 2.75 = -0.21] and intruded with mafics [(2.37 + 0.17 + 0.10) - 2.75 = -0.11]. These model density contrasts provide constraints in explaining the seismic refraction model in terms of a gravity-density analysis.

ADJUSTED SONIC LOG VELOCITIES

Interval velocities were determined seismically by surface shooting and measuring the travel times along the hole, and by sonic logging for six drill holes (Fig. 4). Figure 4 shows only the adjusted sonic log velocities provided by the logging company and averaged over constant velocity intervals. These velocity values are plotted as a function of depth in Figure 6. This separates the holes on the basis of thermal metamorphism as indicated by the amount of mafics included in the column; the unmetamorphosed region is on the left and the metamorphosed region is on the right.

Linear regression lines were calculated to fit the velocity data in Figure 6. Because the velocity data are affected by permafrost to a depth of about 450 m the starting velocity data begin at this depth. Two holes, one in the metamorphosed region and the other in the unmetamorphosed region, penetrate a considerable thickness of Triassic sediments and show that the velocity gradient decreases abruptly in the lower Triassic sediments. Table 3 lists the velocities and gradients shown in Figure 6. The average starting velocity is 2.69 ± 0.61 km/s in the unmetamorphosed region and 3.82 0.06 km/s in the metamorphosed region. The velocity increase of 1.13 km/s is probably due to metamorphism of the sediments and the intrusion of igneous mafic rocks. Some of these rocks were laid down as a volcanic unit (the Strand Fiord Formation) in early Late Cretaceous time (Ricketts et al., 1985). The igneous rock intervals have been noted in Figure 6 by solid lines and usually give a local high velocity.

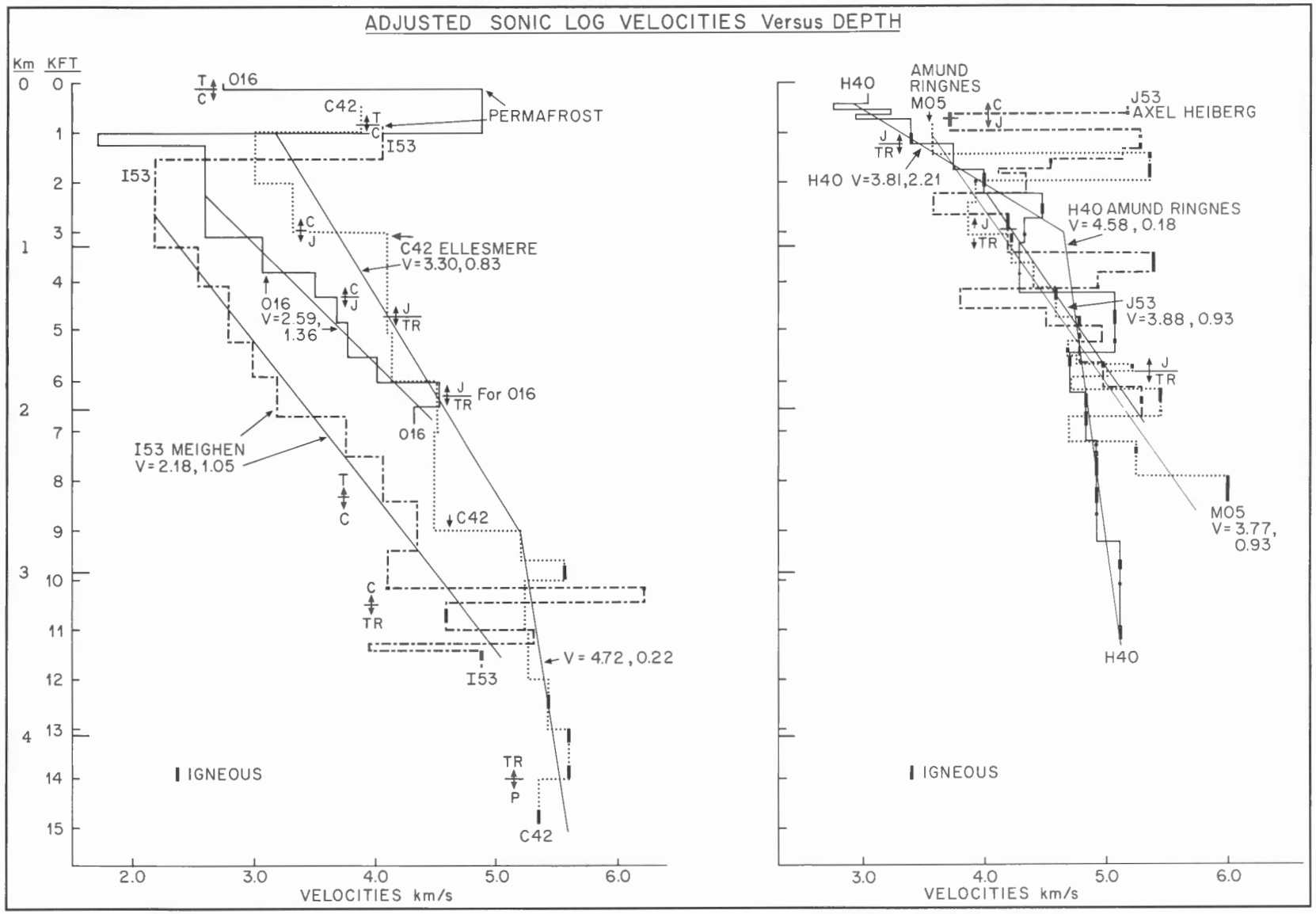

Figure 6. Adjusted sonic log velocities (km/s) and gradients (/s) versus depth for drill holes I53, H40, M05, J53, C42, O16 and J34 which are located on Meighen Island, Axel Heiberg Island, Amund Ringnes Island and Ellesmere Island. Letters T, C, J, TR, P stand for Tertiary, Cretaceous, Jurassic, Triassic and Permian periods, respectively. The three holes on the left and right side were drilled through unmetamorphosed and metamorphosed sediments respectively.

All the sediments (metamorphosed and unmetamorphosed regions) above the lower Triassic have high velocity gradients varying from 0.83 to 2.21/s, whereas lower Triassic sediments have low velocity gradients varying from 0.18 to 0.22/s. These high velocity gradients appear to be unaffected by metamorphism, as they vary between 0.93 and 2.21/s in the metamorphosed zone. The mean velocity gradient for both metamorphosed and unmetamorphosed regions above the lower Triassic is 1.22/s; for the lower Triassic it is 0.20/s.

Seismic model velocities compared with adjusted sonic log velocities

Seismic refraction velocities for sections E_3-I_{29}, B_2-C_4-D_{17} and G_{27}-I_{29} were determined by Asudeh et al. (1989) and are compared to the adjusted sonic log velocities. Section E_3-I_{29} is shown in profile A-A′ in Figure 2. Asudeh et al. (1989) related five velocity regimes to different tectono-stratigraphic sequences from low velocities to high velocities as follows:

1. Unit 5 at the surface, with a starting (initial velocity at the top of a particular sequence) velocity of 2.1 km/s and a velocity gradient of 0.2 to 0.5/s, corresponds with Cretaceous-Tertiary sediments.
2. Unit 4, with a starting velocity of 4.4 to 4.5 km/s at a depth of 2.9 km and a velocity gradient of 0.08 to 0.15/s, corresponds with Cretaceous-Tertiary as well as possibly minor upper Paleozoic-Jurassic sediments.
3. Unit 3, with a starting velocity of 5.0 km/s and a velocity gradient of 0.12/s, underlies unit 5 and is interpreted as predominantly deformed and metamorphosed lower Paleozoic Franklinian strata capped by minor upper Paleozoic-Triassic strata of the Sverdrup Basin sequence, including dense Carboniferous carbonates and/or Cretaceous rocks.
4. Unit 2, with a velocity of 5.8 to 6.0 km/s and a gradient of 0.04 to 0.1/s, underlies units 3, 4 and 5 and is interpreted as undivided crystalline basement composed of deformed and metamorphosed Proterozoic-lower Paleozoic section and underlying "basement" crust.
5. Unit 1, identified only on section B_2-C_{11}-D17 with a velocity greater than 8.0 km/s, is taken as the upper mantle.

Analysis of the adjusted sonic log velocities for six drill holes (Fig. 6, Table 3) show low starting velocities (mean 2.69 km/s in an unmetamorphosed region to 3.82 km/s in a metamorphosed region) below the permafrost layer, with high velocity gradients (1.22/s, much larger than shown by the seismic refraction survey) down to about the mid Triassic; there the gradients decrease abruptly to a mean value 0.20/s, larger than shown by seismic refraction. The velocities for the sediments above the Lower Triassic appear to be affected mainly by the degree of metamorphism, which can increase the starting velocity by as much as 1.13 km/s. The difference (about 150 km) in position of well data and seismic data and different structural, stratigraphic and erosional levels of the top of various sections may also affect the starting velocities. Offshore probably more section is preserved. Age (depth of burial) can also affect the starting velocity (2.18 km/s opposed to 2.59 and 3.30 km/s), as noted between Tertiary and upper Cretaceous sediments (drill holes I-53, Table 3) and Cretaceous, Jurassic and upper Triassic sediments (drill holes 0-16 and C-42, Table 3). The mean velocity of 2.95 km/s, with a mean gradient of 1.10/s for holes 0-16 and C-42, represents the unmetamorphosed Mesozoic sediments of the Sverdrup Basin, whereas a starting velocity of 3.82 km/s and a gradient of 1.36/s represents the metamorphosed sediments of the Sverdrup Basin. The mean starting velocity below the permafrost for mid Triassic sediments and lower is 4.65 km/s (mean of 4.58 and 4.72 km/s, Table 3) and appears to be unaffected by the degree of metamorphism. Thus, these adjusted sonic log velocities for Triassic to Tertiary sediments provide comparisons for the seismic velocity model proposed by Asudeh et al. (1989) and shown in Figure 2. Gradients shown by Asudeh et al. (1989) are generally much lower than those determined from the drill holes and present a problem in relating velocities to lithologies.

The adjusted sonic log velocity of 2.18 km/s for drill hole (I-53) on Meighen Island supports the velocity of 2.1 km/s for Unit 5, which represents Cretaceous-Tertiary sediments of the Arctic Terrace Wedge of the Canadian Arctic Margin Basin. The refraction seismic velocity of 2.1 km/s with a gradient of 0.2/s, if extended to a depth of 2.9 to 4.5 km as shown for line E_3-I_{29} (Fig. 2) for unit 4, would only be 2.68 to 3.00 km/s. These values are much lower than the observed seismic velocities of 4.4 to 4.5 km/s. Table 3 shows that the starting velocities for Sverdrup Basin sediments (above mid-Triassic) are 0.85 km/s [2.95 km/s (mean of drill holes 0-16 and C-42) - 2.1 km/s] higher for unmetamorphosed sediments and 1.72 km/s for metamorphosed sediments (3.82 - 2.1 km/s). If these velocity increases were applied to the bottom velocities of unit 5 of 2.68 and 3.00 km/s at depths of 2.9 and 4.5 km then they would increase to 3.53 and 3.85 km/s in unmetamorphosed sediments and to 4.40 and 4.72 km/s in a metamorphosed region, providing the lower velocity gradient of 0.2/s for the seismic refraction model is used. The drill holes show much larger gradients, which would yield much larger starting velocities at depths of 2.9 and 4.5 km. Thus unit 4 with a velocity of 4.4 km/s probably represents the unmetamorphosed part of the Sverdrup Basin.

Velocities for the metamorphosed part of the Sverdrup Basin are on average 0.87 km/s higher (3.82 km/s for metamorphosed sediments, Table 3 - 2.95 km/s as discussed above). Unit 3 has a higher velocity (5.0 km/s) than unit 4 (4.4 to 4.5 km/s) and is about 3 km shallower (Fig. 2). If the velocity gradient of 0.12/s is used then the starting velocity for the shallower depth would decrease by 0.36 km/s. Thus a metamorphosed unit 4 at a shallower depth would have a velocity of 4.91 to 5.01 km/s. Thus unit 3 probably represents the metamorphosed part of the Sverdrup Basin. This hypothesis is tested in the following gravity-density model analysis.

Unit 2 with a velocity of 5.8 to 6.0 km/s was interpreted by Asudeh et al. (1989) to represent the crystalline basement composed of deformed and metamorphosed Proterozoic-lower Paleozoic section of the Franklinian Basin. The horst part of this unit underlies unit 5 (Fig. 2). The gravity anomaly

over this horst does not appear to give any indication of an uplifted block of dense material. This feature is also investigated in the following gravity-density model analysis.

MAGNETIC ANOMALIES

Aeromagnetic data obtained by the Geological Survey of Canada and the National Geophysical Data Centre were adjusted to the 1975 International Geomagnetic Reference Field. The GSC surveys were flown at a 300 m mean terrain clearance and at a 2 km flight spacing whereas the NGDC survey was widely spaced, including about six profiles in the area of Figure 7. The magnetic field is much more variable than the gravity field (Fig. 3,7). Regions of positive EIA (Fig. 3) have a highly anomalous magnetic character (Fig. 7, amplitudes usually vary between 300 and 750 nanoteslas, with wavelengths much shorter than for gravity). Generally the region on land and immediately offshore is covered by long wavelength, negative magnetic anomalies, probably related to the thick unintruded sediments. On the other hand, where these sediments are intruded with mafic igneous rocks, the magnetic anomalies are much more intense, as observed onshore, and even more, offshore. Magnetic anomalies were not used in the modelling analysis as they are still incomplete regionally but were used qualitatively to emphasize areas that have been affected by volcanism.

MANTLE DEPTHS

Water and surface topography were compensated by variations in crustal thicknesses, according to a model of Airy isostasy for the Arctic discussed by Sobczak and Halpenny (1990a,b). The depths to the top of the mantle, which were assumed to be 30 km at the shoreline,are shown for the survey area in Figure 8 and along profiles A-A′, B-B′ and C-C′ discussed later in this report.

Crustal thicknesses shown in Figures 9 and 10 were set to a depth of 25 km, as determined seismically by Asudeh et al. (1989) along profile B_2-C $_4$-D_{17}, which would intersect profile A-A′ at shot point E. Model gravity-density analysis showed that 14 km of mantle anti-root with a crust-mantle density contrast of 0.4 Mg/m^3 was required to compensate for the mass deficiency of the sediments. A further adjustment to this mantle surface (Fig. 11) was made for the effect of water and the IA relationships which were involved in determining the EIA. These adjustments place the mantle surface at the seaward end of profile A-A′ at a depth of 15 km and at the landward end at a depth of 40 km. The mantle surface on the seaward end of the profile is at the base of the sedimentary sequence, suggesting that this is the maximum amount of sediments. In all likelihood thinner sediments, a thin crust and a deeper mantle surface probably exists seaward of shot point E and not as assumed and shown in the model of Figures 9 and 10 in which the thicknesses of the sediments were generally taken to be the same as at shot point E_3. Until seismic crustal depths are determined on the seaward end of the profile, further gravity-density modelling will be inefectual.

PROFILE ANALYSIS, PROFILE A-A′

The crustal section along profile A-A′ (Fig. 2) was determined by comparing the observed gravity as outlined in the enhanced isostatic anomaly (Fig. 3) with the calculated gravity effects for models constrained by data on densities and adjusted sonic log velocities discussed earlier, by the seismic refraction model between E_3-I_{29} proposed by Asudeh et al. (1989), and by the geology on land compiled by Thorsteinsson and Trettin, (1971). Computations of the gravity effects were made using a DEC VAX version of MAGRAV (Rupert, 1987). Mass deficiency of the sedimentary basins was compensated by the excess mass of the mantle antiroots determined seismically (Asudeh et al., 1989) to be at a depth of 25 km below the seaward end of profile E_3-I_{29}. The thicknesses of the Canadian Arctic Margin Basin and Sverdrup Basin landward and seaward of profile E_3-I_{29} were adjusted to fit with the EIA observed anomaly. Certain questions were addressed as follows:

1. Does the seismic model explain the gravity anomaly if appropriate densities are used?
2. What are the likely basin sequences for the model?
3. Does the horst part of unit 2 represent material similar to the rest of Unit 2 underlying units 3 and 4?

The models in Figure 9 show body 4 to have a density contrast of -0.09 Mg/m^3 (option 1), similar to the underlying Franklinian Basin sediments, whereas option 2 shows body 4 with a density contrast of -0.38 Mg/m^3, similar to the adjacent Sverdrup Basin sediments on either side. The gravity over body 4 (option 1, Fig. 9) has a calculated relative positive anomaly difference of over 30 mGal with respect to the observed EIA, whereas an excellent match is obtained in option 2. Thus the model in option 2 best fits the data, showing a simple regional structure of overlying basins.

Figure 10 shows further density contrasts superimposed on the model shown in Figure 9 in order to get the calculated and observed EIA to fit to within 3 mGal. These superimposed effects are probably due to metamorphism and mafic intrusions. Increase in density of Sverdrup Basin sediments by metamorphism determined from drill holes was found to be as large as 0.17 Mg/m^3 (Fig. 5, Table 2). Bodies 8 and 9 of Figure 10 show a general increase in density contrast (from 0.02 to 0.04 Mg/m^3) in the Phanerozoic sediments from the seaward to the landward ends of profile A-A′. This density increase probably represents partial metamorphism: about 12 to 24% in the Sverdrup Basin sediments, and about 22 to 44% for the Franklinian Basin sediments, with respect to metamorphism density increases found in the drillhole data. Body 10, located at the landward end of profile E_3-I_{29}, shows a further increase in density contrast of 0.05 Mg/m^3. This represents an increase of a little over 50% in metamorphism as determined from drill holes. Body 11 shows an area where the increase would be +0.08 Mg/m^3; in the Sverdrup Basin layer this represents 70% of the metamorphism sampled in the drill holes, but in the Franklinian Basin layer it involves total metamorphism and intrusion of mafic rocks. Bodies 12 and 13 represent areas of greatest metamorphism and mafic intrusion, as evidenced by exposed mafic rocks a few

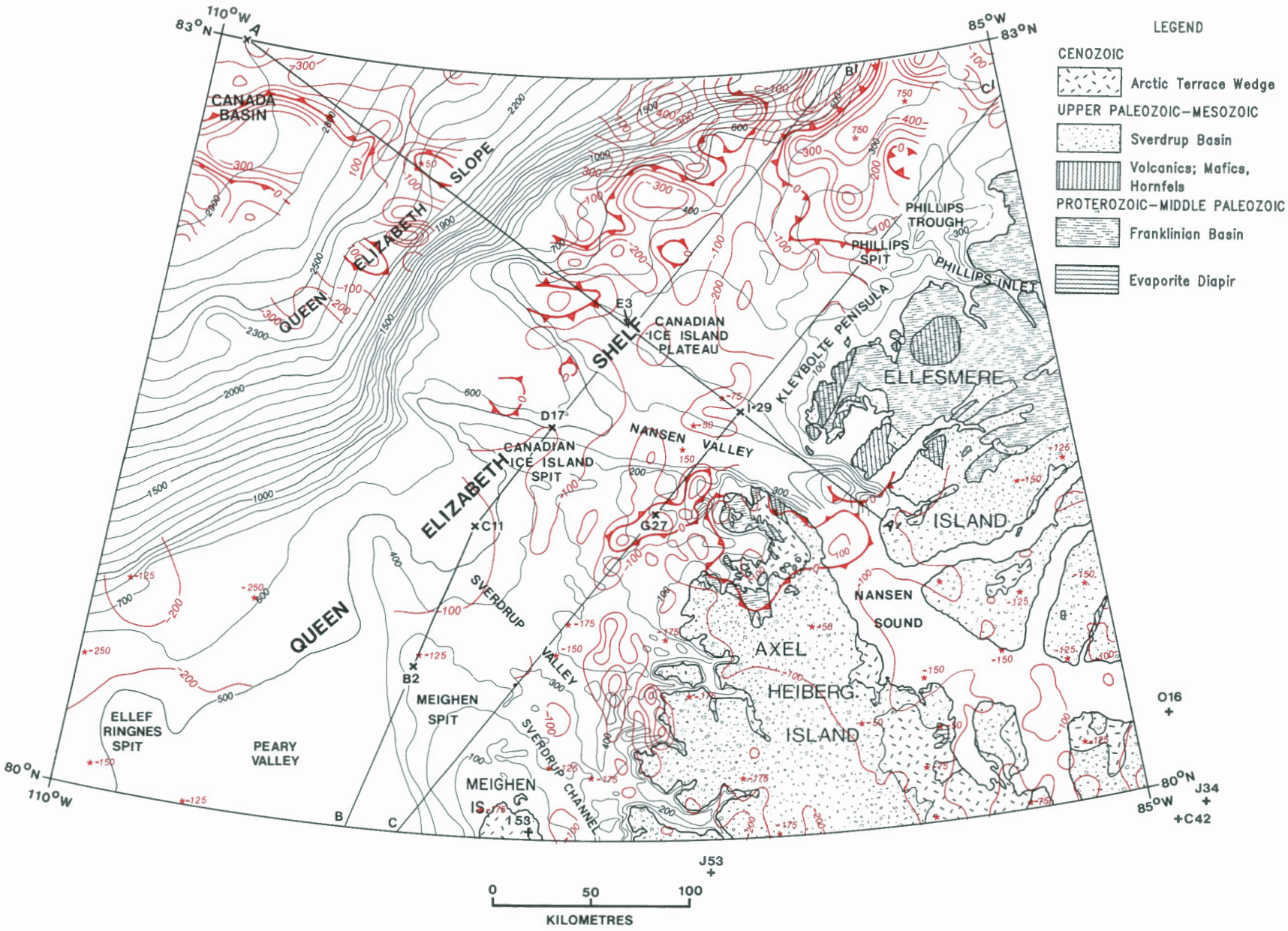

Figure 7. Magnetic anomalies are shown in red. Contour interval 100 nanoteslas. Zero anomaly contour is heavier with barbs on the negative anomaly side.

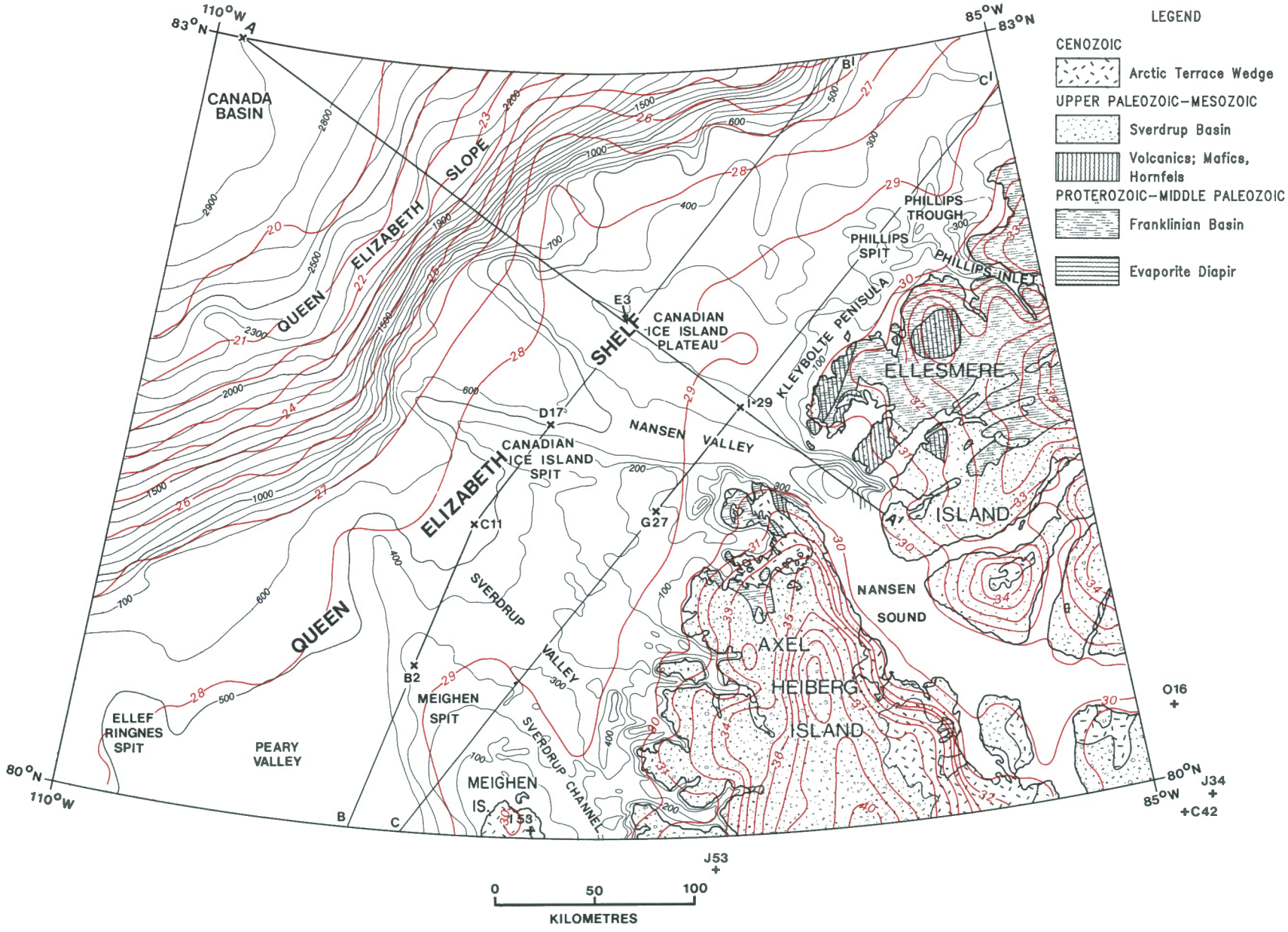

Figure 8. Crustal thicknesses in kilometres with a contour interval of 1 km are shown in red. These thicknesses were determined from the rock equivalent topography obtained for the Arctic by Sobczak and Halpenny (1990a,b).

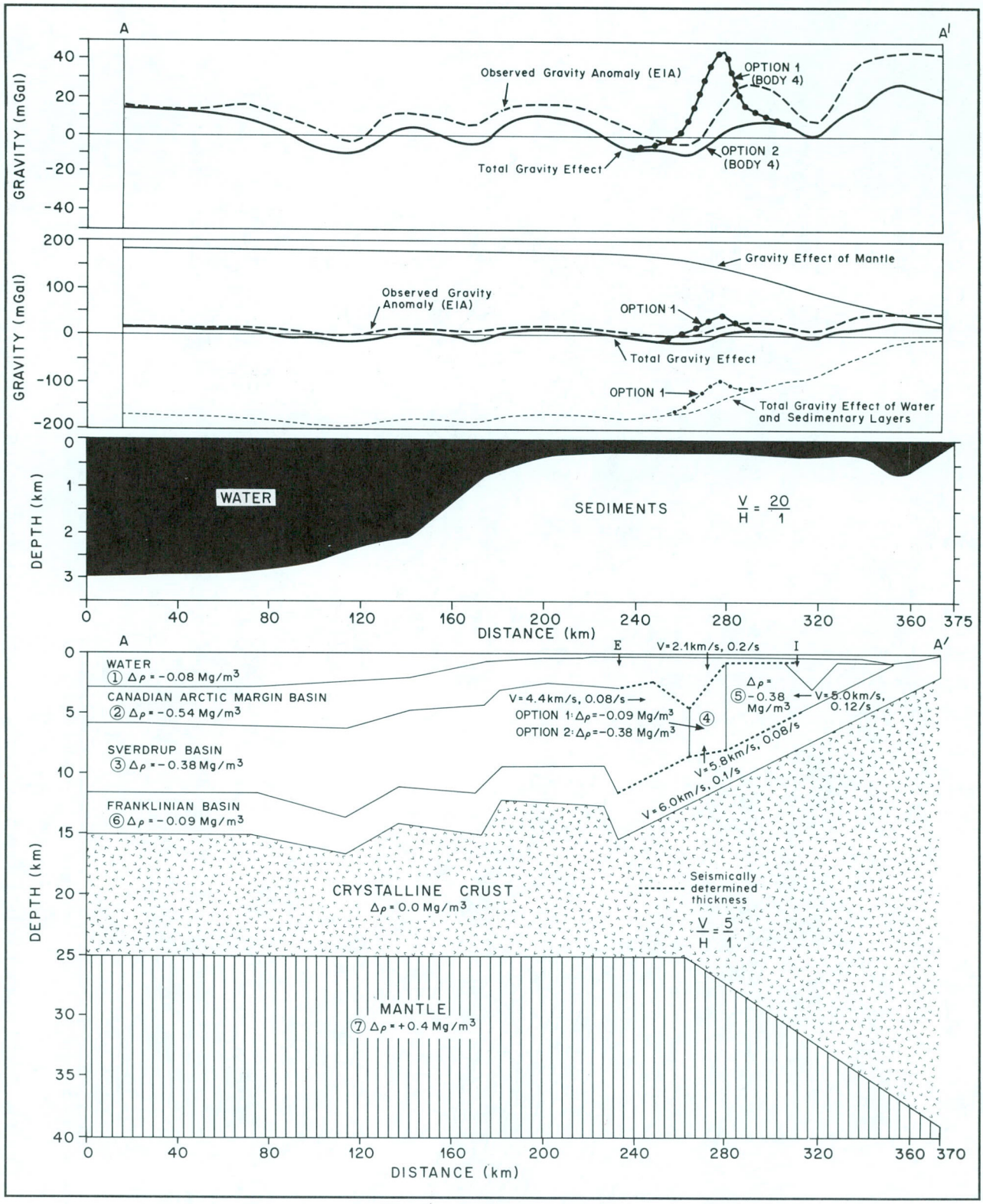

Figure 9. Profile A-A′ showing observed gravity anomaly (EIA), total gravity effect of the water and sedimentary layers, gravity effect of the mantle and total gravity effect for the section to a depth of 39 km. The seismic refraction model is shown by dashed lines between E_3-I_{29}. The water layer (1) has a density contrast of -0.08 Mg/m^3. This value was obtained by using a density of 2.67 Mg/m^3 for sea water in the EIA minus the density for the assumed standard crust (2.75 Mg/m^3). Density contrasts for the Canadian Arctic Margin Basin, Sverdrup Basin and Franklinian Basin, taken from Table 2, are shown. Depth to the top of the mantle was taken at 25 km at the seaward end of profile E_3-I_{29} as discussed by Asudeh et al. (1989). The density contrast for body 4 was altered from -0.09 (Option 1) to -0.38 Mg/m^3 (Option 2).

kilometres to the northeast of profile A-A′ on land (Thorsteinsson and Trettin, 1971a,b,c,d), and delineated by a large positive EIA (+45 mGal, Figs. 2, 3).

Body 4 (Fig. 9), interpreted seismically (Asudeh et al., 1989) as a horst structure representing part of the underlying undivided crystalline basement of the Franklinian Basin (unit 2) is an enigma. Velocities are high (1 to 1.5 km/s higher than the adjacent sediments), varying from 5.8 to 6.0 km/s, and appear to represent Franklinian Basin rocks, but the densities are more or less normal, similar to the Sverdrup Basin sediments on either side (bodies 3 and 5, Fig. 9). This feature lies on the steep gravity gradient between the gravity low to the northwest and the high to the southeast, and on the landward flank of a thick (4.5 km) basin (Canadian Arctic Margin Basin) to the northwest and very thin (700 m) basin to the southeast. Mafic intrusions can give the higher velocities but they are also very dense. Sobczak and Overton (1984) discovered velocity increases (pull ups) with mass deficiencies in the Sverdrup and Franklinian basin sediments which they interpreted as being the effects of evaporites. Grant and West (1965, p. 7, 8) recognized, on the basis of

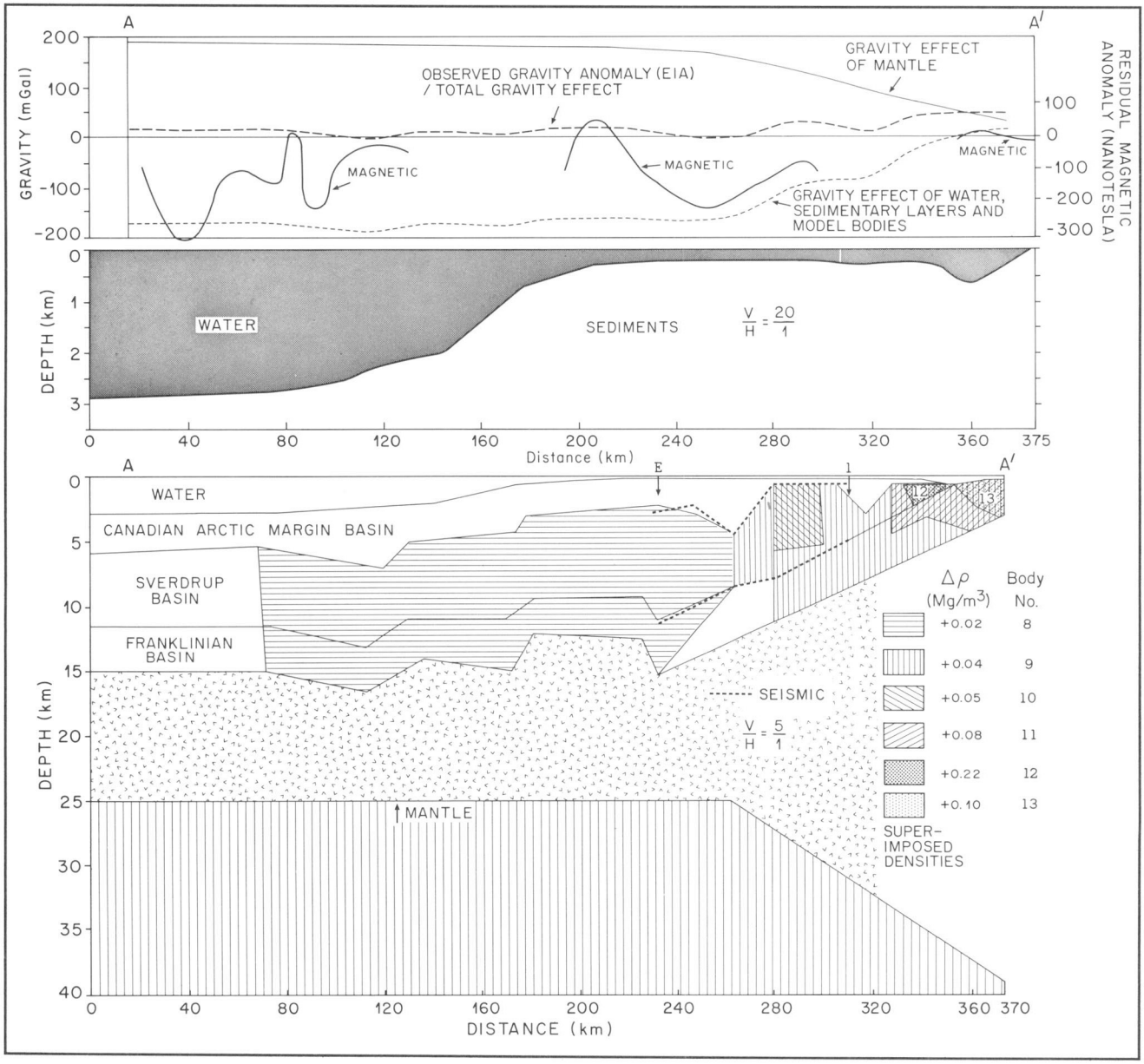

Figure 10. Profile A-A′ showing observed gravity anomaly (EIA), total gravity effect of the water and sedimentary layers plus density increases due to metamorphism and mafic intrusives (bodies 8-13), gravity effect of the mantle and total gravity effect for the section to a depth of 39 km. The seismic refraction model is shown by dashed lines between shot points E_3 and I_{29}. Density contrasts (Mg/m^3) were superimposed on the section shown in Figure 9. The total gravity effect is equal to the observed gravity anomaly (EIA) to within 3 mGal and therefore only a single curve is shown.

seismic velocities, five categories of earth materials, which are, in order of increasing longitudinal-wave velocity: (1) alluvium, soil, unconsolidated sediments; (2) sandstone and shale; (3) carbonates; (4) granites and other crystalline igneous and metamorphic rock; and (5) salt. Using Birch's (1942) Handbook of Physical Constants, they found salt to have the highest velocity, varying from 4.29 to 7.62 km/s with a mean value of 5.95 km/s. A similar high velocity has been found for body 4 (unit 2) by Asudeh et al. (1989). While this velocity is possible from other combinations of igneous and sedimentary rocks, gravity-density analysis suggests that body 4 (Fig. 10) has a low mean density of 2.41 Mg/m^3, which is only 0.10 Mg/m^3 higher than that typical for evaporites. This suggests that perhaps some mafic igneous rocks are also included in body 4, which consists primarily of evaporites. Large evaporite deposits are found in the Sverdrup and Franklinian basins as discussed by Sobczak et al. (1970) and Balkwill (1983).

A possible ratio between mafic and evaporite rocks was estimated. The cross-sectional area of body 4 is 90 km^2, and the density contrast is -0.44 Mg/m^3 (2.31-2.75) for evaporites and 0.16 Mg/m^3 (2.91-2.75) for mafic rocks. The cross-sectional area equals 75 km^2 for evaporites and 15 km^2 for mafics, resulting in a ratio of evaporites to mafics of 5 to 1.

PROFILE B-B′

Analysis of gravity along profile B-B′ (Fig. 12) constrained by the seismic refraction model shown between B_2-C_{11}-D_{17} outlines the amount of uncompensated sediments to the southwest and the region of metamorphism to the northeast. Only a slight modification to bodies 6 and 14 was required, as shown by the dashed lines (seismic) and solid lines (gravity). However, bodies 6 and 14 have a higher velocity (6.2 km/s), lie at a shallower depth (9.2 km) and have a lower density (2.57 Mg/m^3) than the Franklinian Basin sediments to the southwest (velocity 6.0 km/s, depth 12 km and density 2.66 Mg/m^3). Again, we are suggesting that parts of bodies 6 and 14 consist of evaporites that account for the higher velocity and lower density contrast. Body 7 has the same density as body 5 but a higher velocity (6.2 km/s). Perhaps evaporites are involved in this body as well, but the gravity effect of low density evaporites may be offset by dense mafic igneous rocks, as noted by the higher densities in the adjacent bodies 10 and 12. Body 10 (density contrast+0.02 Mg/m^3) indicates a mild increase in metamorphism of the Sverdrup and Franklinian Basin sediments as shown in Figure 10, whereas body 12 (density contrast +0.10 Mg/m^3) may indicate a region of mafic rocks. Relative positive magnetic anomalies are also observed over parts of bodies 10 and 12, possibly indicating small quantities of local

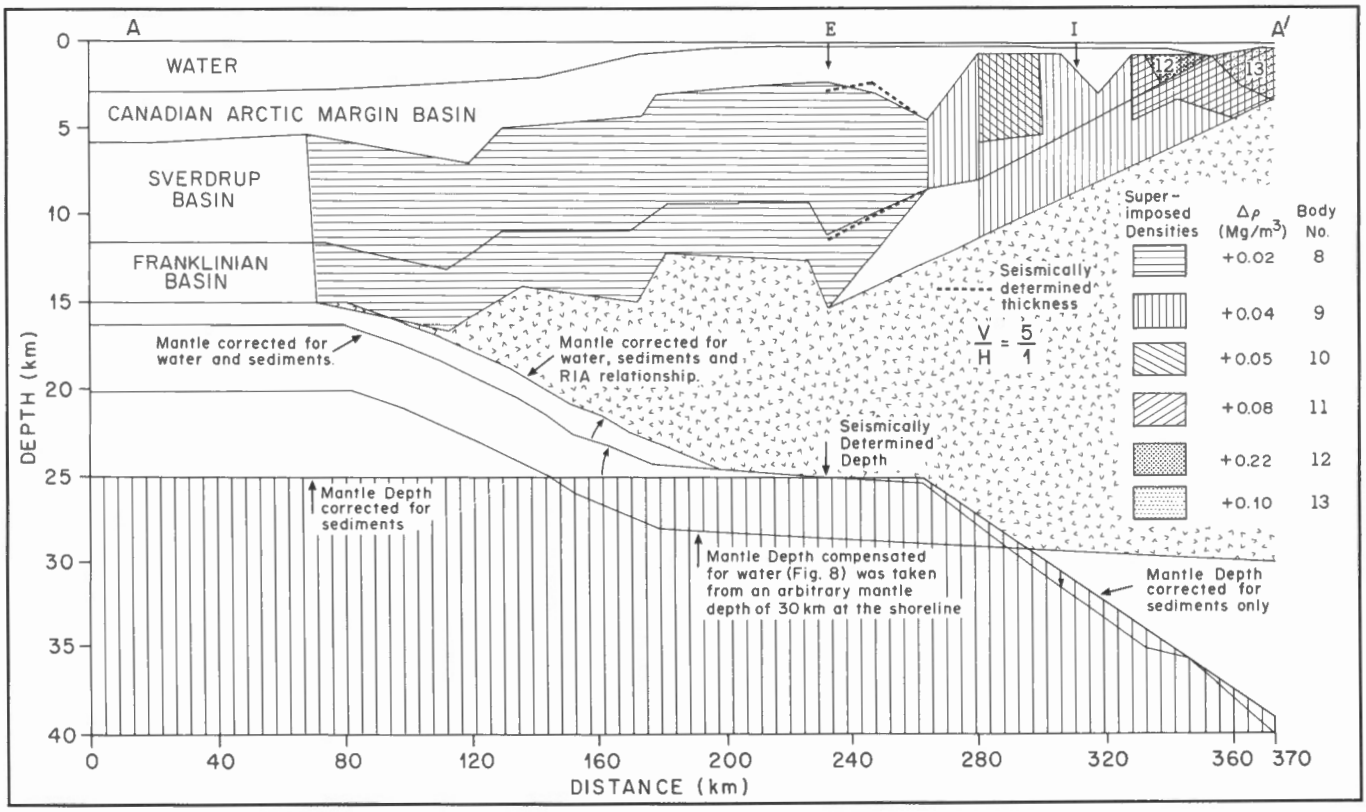

Figure 11. Corrected crustal thicknesses along profile A-A′ based on the model shown in Figure 8. Arrows at the crust-mantle surface point to the corrected depth to the top of the mantle just below the crustal rocks which are patterned.

mafic intrusions. On the other hand, the negative magnetic anomalies probably outline areas free of mafic rocks within the zone of metamorphism.

The relative gravity anomaly high (+5 mGal) at shot point B_2 is at the eastern end of the large positive shelf edge anomaly (+80 mGal) discussed earlier. This anomaly may be explained by an uncompensated lens of sediments up to 800 m thick (Fig. 12). If an equivalent water layer existed, prior to sediment deposition, it may have been compensated by a mantle upwelling, as shown in Figure 12, or the strength of the crust could have carried this small load of water.

The depth to the surface of the mantle was adjusted for the effect of the water (Fig. 12). In the gravity model analysis 14 km of mantle anti-root compensates for the mass deficiency of the sediments. Additional corrections are made for mantle depths shown in Figure 8 and are applied to the mantle surface (Fig. 12).

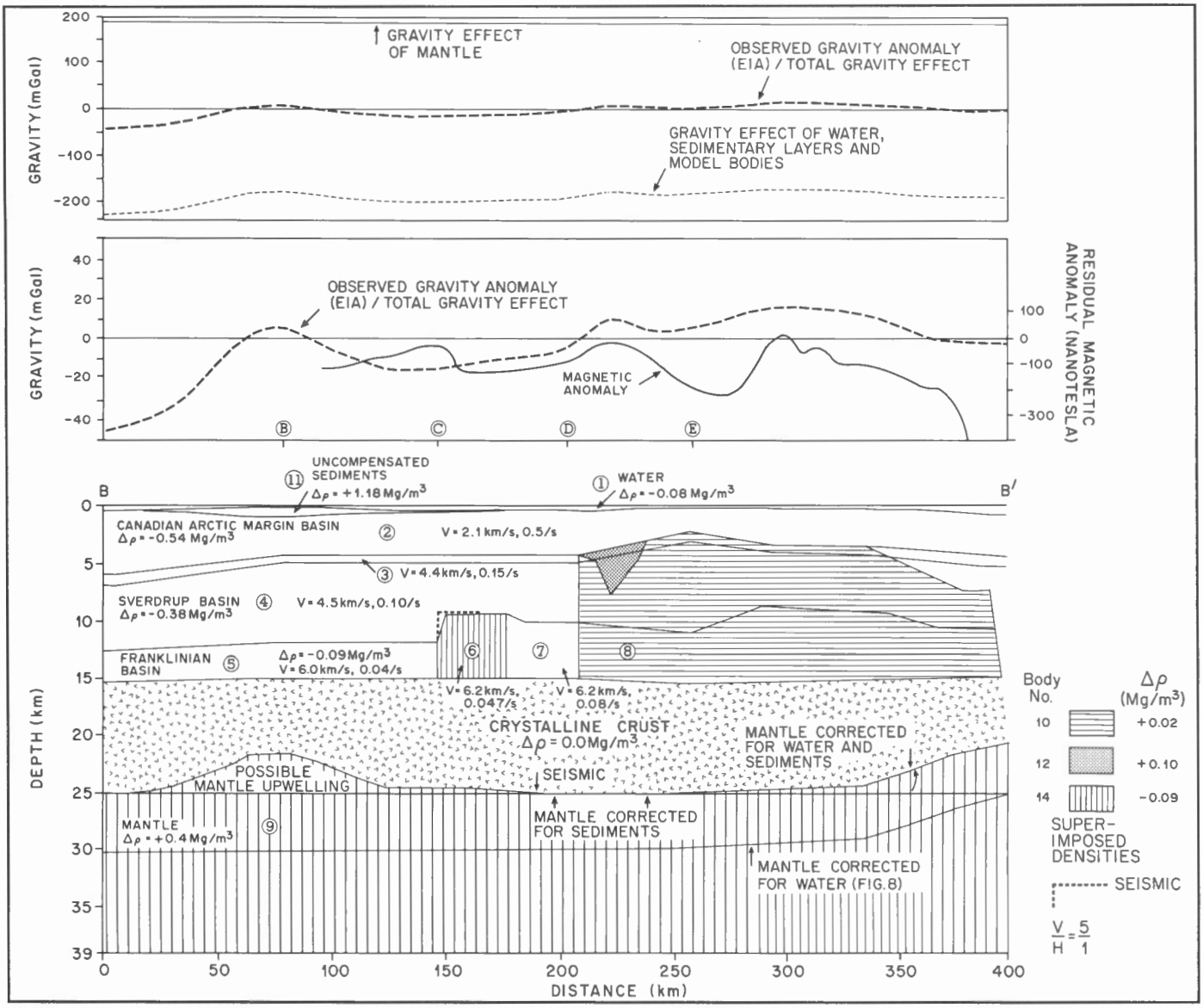

Figure 12. Profile B-B′ showing observed gravity anomaly (EIA), total gravity effect of the water and sedimentary layers (bodies 1-8), plus superimposed density changes due to metamorphism (body 10), mafic intrusives (body 12) and zone of evaporites within Franklinian Basin Sediments (body 14), gravity effect of the mantle and total gravity effect for the section to a depth of 39 km. The seismic refraction model where it differs from the gravity model is shown by dashed lines between B_2-C_{11}-D_{17}. The total gravity effect is equal to the observed gravity anomaly (EIA) to within 3 mGal. These are shown as a single curve in the upper and lower diagram. The residual magnetic anomalies are also shown. The final mantle surface was adjusted for the water and sediments (Fig. 12) and is shown by an arrow. Body 11 represents an uncompensated portion of sediments of the Arctic Terrace Wedge. Prior to the deposition of these sediments body 11 was probably water which may have been compensated by a mantle upwelling (body 13).

PROFILE C-C′

Analysis of gravity along Profile C-C′ (Fig. 13), using the seismic model between shot points G_{27} and I_{29} for partial control, shows a fairly complex crustal section. The Canadian Arctic Margin Basin (Arctic Terrace Wedge) thickens from 700 m to 5 km to the southwest. Between shot points G_{27} and I_{29}, it appears to be thicker by a few hundred metres towards I_{29} than shown seismically, and to the northeast this basin thickens to 3.5 km; it is on strike with the gravity anomaly low shown between shot points E_3 and I_{29} (Profile A-A′, Fig. 10) where this basin thickens to 4.5 km. The Sverdrup and Franklinian basin sediments appear to be slightly metamorphosed in the vicinity of shot point G_{27} (body 7 with a density contrast of +0.02 Mg/m^3) and increased metamorphism in the vicinity of shot point I_{29} (body 8 with a density contrast of +0.04 Mg/m^3). Also, in these areas increased mass excesses are applied to bodies 10 and 6 by assigning them a density contrast of +0.10 Mg/m^3, probably due to mafic intrusions. Magnetically, this region is quite anomalous, having much shorter wavelengths than those observed in the gravity field, probably reflecting the

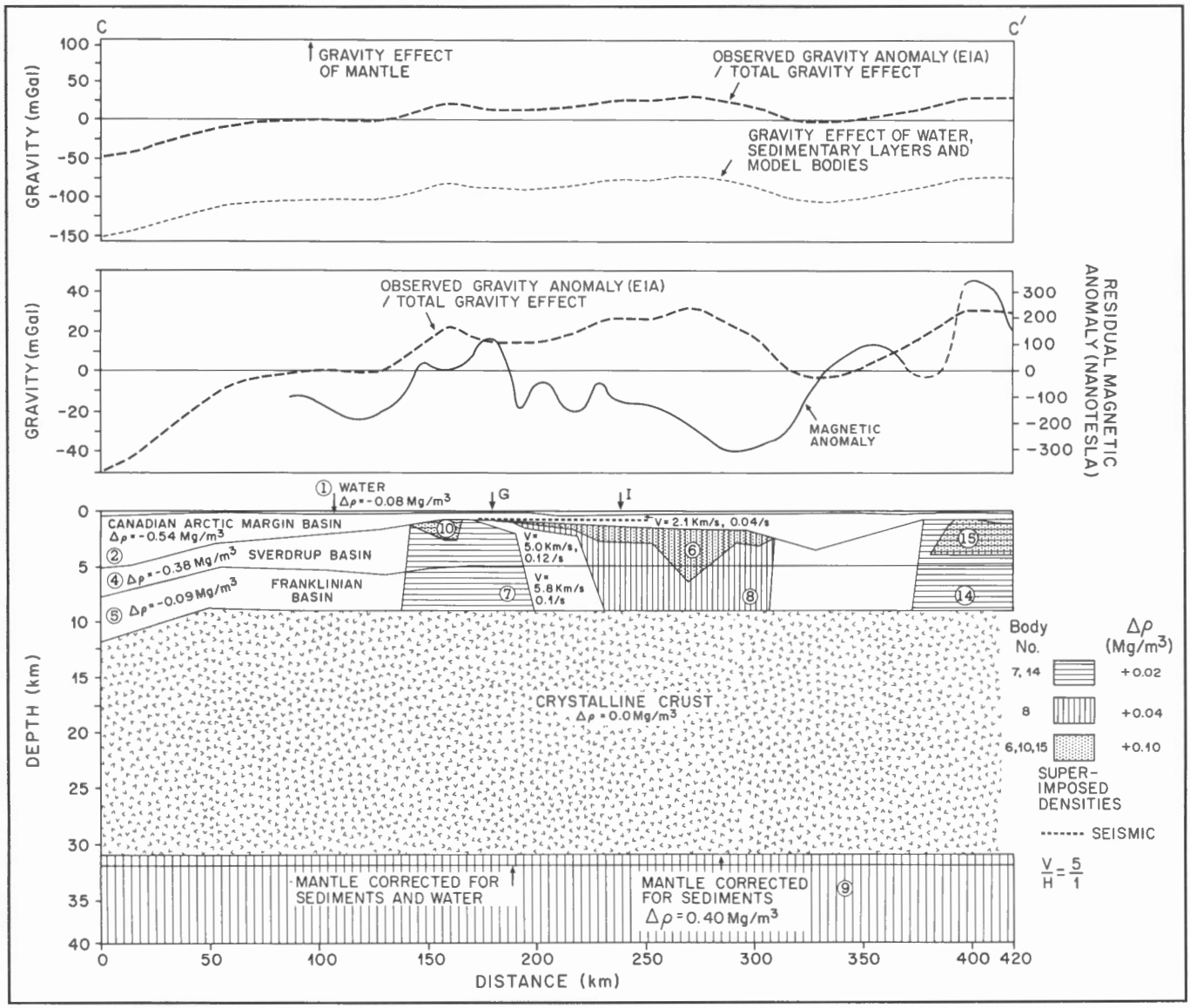

Figure 13. Profile C-C′ showing observed gravity anomaly (EIA), total gravity of the water and sedimentary layers (bodies 1-5), plus superimposed density changes due to metamorphism (bodies, 7, 8, 14), mafic intrusives (bodies 6, 10, 15), gravity effect of the mantle and total gravity effect for the section to a depth of 39 km. The seismic refraction model is shown by dashed lines between G_{27} and I_{29}. In the gravity-density model the Canadian Arctic Margin Basin is made thicker, in keeping with Figure 10. The total gravity effect is equal to the observed gravity anomaly (EIA) to within 3 mGal. It is shown as a single curve in the upper and lower diagram. The residual magnetic anomalies are also shown; these may be dubious northeast from shotpoint I_{29} to C′. The mantle surface was lowered by 1 km from 31 to 32 km depth in order to correct for the effect of water and topography shown in Figure 12.

heterogeneity of the mafic intrusions. Seismically, the velocity (5.0 km/s, 0.12/s) for Sverdrup Basin sediments is higher than for unmetamorphosed sediments (4.4 to 4.5 km/s, 0.08-0.15/s, Fig. 9), suggesting a higher degree of metamorphism. A similar metamorphosed and intruded zone is interpreted to be present at the northeast end of the profile (C-C′).

The depth to the surface of the mantle was lowered from a depth of 31 km to 32 km (Fig. 13). This adjustment corrects for the effect of water and topography noted in Figure 8.

SUMMARY

The structure and character of the continental margin have been investigated using geological and geophysical data offshore of Axel Heiberg and northwestern Ellesmere islands. Control for sedimentary and crustal thicknesses along parts of profiles A-A′ (Fig. 10, 11), B-B′ (Fig. 12) and C-C′ (Fig. 13) was obtained from seismic refraction lines (Asudeh et al., 1989). Lithologies, densities and interval velocities were obtained from drill holes on the Queen Elizabeth Islands. Surface geology was obtained from maps compiled by Thorsteinsson and Trettin (1971a,b,c,d). Magnetic anomalies apparently emphasize areas that have been affected by volcanism. The gravity analysis utilized these data in determining gravity-density structural sections along these profiles and in turn provides the control to discuss more regional aspects of the EIA anomalies shown in Figure 3 away from the actual lines.

The EIA, except for the large shelf edge anomaly (maximum +80 mGal), outlines the western third of the map as negative and the eastern part as mostly positive. The area of negative anomalies delineates a thick, (15 km) unmetamorphosed, sedimentary sequence containing evaporites at the base of the Franklinian Basin located near the centres of the local gravity lows, such as that near shot point C_{11} (Fig. 12), and on the landward flanks of the Canadian Arctic Margin Basin between shot points E_3 and I_{29} (Fig. 10). The large shelf edge anomaly over this thick combined sedimentary sequence may represent an 800 m thick lens of young uncompensated sediments. This extensive EIA low north of the Sverdrup Rim, defined as a positive tectonic element by Balkwill (1983), crosses the rim southward along Peary Valley (Fig. 3) and Prince Gustaf Adolf Sea southwest of Ellef Ringnes Island where it merges with the extensive low over the western part of the Sverdrup Basin (Sobczak and Halpenny, 1990a,b) which contains significant amounts of hydrocarbons mainly in the form of natural gas.

A narrow, northeast trending extension of this low extends from the seaward end of the seismic refraction line E_3-I_{29} to Phillips Trough. A thickened (4.5 km) Canadian Arctic Margin Basin was found seismically in the location of this gravity low. This thickened basin explains this gravity low. Also in this location, a shallow, high velocity 5.8 to 6.2 km/s structure was found. Asudeh et al. (1989) explained this structure in terms of an uplifted basement horst of the Franklinian Basin. However, the gravity-density analysis does not support this concept, as there is no relative gravity high associated with it. Instead, we propose the Sverdrup and Franklinian basins are continuous through this high velocity feature, which is explained by a mixture of metamorphosed sediments heavily intruded with evaporites. This accounts for the higher velocities and normal densities noted in this analysis.

It is suggested that evaporites, as they were heated and were intruded by mafics, migrated updip to the location of body 4 (Fig. 9) to form a wall. If the steep gravity gradient is its signature, then this evaporite wall extends from the south midway between Meighen Island and Axel Heiberg Island (98°W), due north from latitude 80°N to about 81°15'N then northeast through line E_3-I_{29}, as indicated in Figure 2 to about 93°W 81°05'N. This wall of evaporites may be a result of volcanism and may not necessarily be related to a rifting process of the Canadian Polar Margin.

The EIA highs in Figure 3, which cover most of the eastern two thirds of the map, are of variable magnitudes and can be explained by various degrees of metamorphism and the intrusion of mafics within the sediments of the Sverdrup and Franklinian basins. Data from drill holes, where mafics are intruded, show that metamorphism of the sediments can increase their density by 0.17 Mg/m^3 for Sverdrup Basin sediments and 0.09 Mg/m^3 for Franklinian Basin sediments. In the region of the profiles, metamorphism usually accounts for about 0.02 to 0.04 Mg/m^3 density increase. This increase is much lower than for areas where mafics are common in the stratigraphic column. The greater concentration of these mafics appear to be near shore or onshore as indicated in Figure 10 (bodies 12, 13). Line C-C′ (Fig. 13, bodies 6, 10, 15), which is closer to shore than line B-B′ (Fig. 12, body 12), shows a greater abundance of mafics.

The total thickness of the sediments appears to be about 15 km along the outer shelf and slope and gradually thins to about 3 km at the shore (profile A-A′, Fig. 10) where the Sverdrup Basin sediments either are very thin or absent and the Franklinian Basin sediments are exposed. This thinning of the sediments probably represents the shoreward side of the northeastward extension of the Sverdrup Rim as shown by Sobczak et al. (1986, their Fig. 1).

Crustal thinning seaward is best shown in Figure 11 where crustal thicknesses vary from 40 km at the shore to 15 km below the Canada Basin. The model shows the maximum amount of sediments below the Canada Basin, as no independent seismic depth control was available in this location. In the model analysis similar sediment thicknesses were proposed below the Canada Basin as indicated near the seaward side of seismic line E_3-I_{29}. In all probability the sediments are thinner below the Canada Basin than shown.

CONCLUSIONS

A huge sedimentary basin exists offshore of the Queen Elizabeth Islands; the northeastern part has been thermally metamorphosed to various degrees and intruded by mafics whereas the southwestern part has been unaffected. Considering the hydrocarbons that have been found to the south of the Sverdrup Rim in the Sverdrup Basin, which has largely

been unaffected by volcanism, there is a strong probability of hydrocarbon occurrence to the north of the Sverdrup Rim in the areas of negative EIA.

EIA have proven to be very useful in depicting anomalous areas in the transition zones between continental and oceanic crusts. They allow us to identify areas affected by volcanism, areas with evaporites, and to determine sedimentary thicknesses below the shelf and slope. This type of anomaly appears to be very useful in interpretation of gravity data in areas with large topographic variations.

It is suggested that the shallow, high velocity zone found by Asudeh et al. (1989) between shot points E_3 and I_{29} may not be an uplifted basement structure but an evaporite zone with possible mafic intrusions. Similarly it is suggested that the higher velocity zone between shot points C_{11} and D_{17} may be a region of evaporites.

Crustal thicknesses vary from 40 km at the shore to 15 km below the Canada Basin.

ACKNOWLEDGMENTS

We would like to thank the personnel of the Polar Continental Shelf Project and their air crews from Bradley and Quasar for their support; J. Davidson and M. Wright of the Atlantic Geoscience Centre for providing SYLEDIS navigation and for checking us out on its use; D. Forsyth, R. Schiemann, J. Thomas and A. Overton for dynamite and technical support; and P. Robertson of Canada Oil and Gas Lands Administration Division of the Department of Indian and Northern Development for providing drill hole data in the Queen Elizabeth Islands. Thanks are also extended to M.D. Thomas, J. Weber, R. Stephenson, D. Forsyth, T. Overton, M. Drury and D. O'Dowd for comments on the manuscript, to E. Maahs, G. MacLeod and L. Campbell for drafting the diagrams, and to R. Delaunais for photography work.

REFERENCES

Airy, G.B.
1855: On the computation of the effect of the attraction of the mountain-masses, as disturbing the apparent astronomical latitude of stations in geodetic surveys; Philosophical Transactions of the Royal Society of London, v. 145, p. 101-104.

Asudeh, I., Forsyth, D.A., Stephenson, R., Embry, A., Jackson, H.R., and White, D.
1989: Crustal structure of the Canadian polar margin; Part 1; Canadian Journal of Earth Sciences, v. 26, p. 853-866.

Balkwill, H.R.
1983: Geology of Amund Ringnes, Cornwall and Haig-Thomas islands, District of Franklin; Geological Survey of Canada, Memoir 390, 76 p.

Birch, F.
1942: Handbook of Physical Constants; edited by F. Birch, Geological Society of America, Special Paper 36, 325 p.

Embry, A.F. and Osadetz, K.G.
1988: Stratigraphy and tectonic significance of Cretaceous volcanism in the Queen Elizabeth Islands, Canadian Arctic Archipelago; Canadian Journal of Earth Sciences, v. 25, p. 1209-1219.

Goodacre, A.K., Grieve, R.A.F., and Halpenny, J.F.
1987: Isostatic Gravity Anomaly Map of Canada; Geological Survey of Canada, Canadian Geophysical Atlas, Map 4, scale 1:10 000 000.

Grant, F.S. and West, G.F.
1965: Interpretation Theory in Applied Geophysics; McGraw-Hill Book Company, New York, New York, 583 p.

Johnson, G.L., Monahan, D., Gronlie, G., and Sobczak, L.W.
1979: General Bathymetric Chart of the Oceans, Arctic Ocean; Canadian Hydrographic Service, Chart 5.17.

Larochelle, A., Black, R.F., and Wanless, R.K.
1965: Paleomagnetism of the Isachsen diabasic rocks; Nature, v. 208, p. 179.

McGrath, P.H. and Fraser, I.
1987: Magnetic Map of Arctic Canada; Geological Survey of Canada, Map 1512-A.

Pelletier, B.R.
1964: Development of submarine physiography in the Canadian Arctic and its relation to crustal movements; Bedford Institute of Oceanography, Dartmouth, Nova Scotia, Report BIO 64-16, p. 1-45.

Perry, R.K., Fleming, H.S., Weber, J.R., Kristoffersen, Y., Hall, J.K., Grantz, A., Johnson, G.L., Cherkis, N.Z., and Larsen, B.
1986: Bathymetry of the Arctic Ocean; Williams and Heintz Map Corporation, Capital Heights, MD. 20743, Map and Chart Series MC-6.

Ricketts, B.D. and McIntyre, D.J.
1986: The Eureka Sound Group of eastern Axel Heiberg Island: new data on the Eurekan Orogeny; *in* Current Research, Part B, Geological Survey of Canada, Paper 86-1B, p. 405-410.

Ricketts, B., Osadetz, K.G., and Embry, A.F.
1985: Volcanic style in the Strand Fiord Formation (Upper Cretaceous), Axel Heiberg Island, Canadian Arctic Archipelago; Polar Research, v. 3, p. 107-122.

Rupert, J.
1987: DEC VAX version of MAGRAV; Geological Survey of Canada, Geophysics Division, Internal Report 87-7, p. 1-18.

Simpson, R.W., Jachens, R.C., Saltus, R.W., and Blakely, R.J.
1986a: Isostatic Residual Gravity, Topographic, and First-vertical-derivative Gravity Maps of the Conterminous United States; Department of the Interior, Unites States Geological Survey, Map GP-975.

Simpson, R.W., Jachens, R.C., Blakely, R.J., and Saltus, R.W.
1986b: A new isostatic residual gravity map of the conterminous United States with a discussion on the significance of isostatic residual anomalies; Journal of Geophysical Research, v. 91 (B8), p. 8348-8372.

Sobczak, L.W.
1975a: Gravity anomalies and passive continental margins, Canada and Norway; *in* Canada's Continental Margins, edited by C.J. Yorath, E.R. Parker, and D.J. Glass, Canadian Society of Petroleum Geologists, Memoir 4, p. 743-761.
1975b: Gravity and deep structure of the continental margin of Banks Island and Mackenzie Delta; Canadian Journal of Earth Sciences, v. 12, p. 378-394.
1978: Gravity from 60°N to the North Pole; *in* Arctic Geophysical Review, edited by J.F. Sweeney, Department of Energy, Mines and Resources, v. 45, p. 67-73.

Sobczak, L.W. and Halpenny, J.F.
1990a: Isostatic and enhanced isostatic gravity anomaly maps of the Arctic; Geological Survey of Canada, Paper 89-16, 10 p.
1990b: Gravity anomaly maps of the Arctic (free-air, Bouguer, isostatic and enhanced isostatic); Marine Geology, Special Issue on Arctic Geoscience, v. 93, no. 1-4, p. 15-41.

Sobczak, L.W. and Overton, T.
1984: Shallow and deep crustal structure of western Sverdrup Basin; Canadian Journal of Earth Sciences, v. 21, p. 902-919.

Sobczak, L.W. and Schmidt, M.
1985: Gravity survey along the seismic refraction line from Ice Island, N.W.T.; Department of Energy, Mines and Resources, Earth Physics Branch, Internal Report No. 85-15, Ice Island Contribution No. 3, p. 1-5.

Sobczak, L.W. and Sweeney, J.F.
1978: Bathymetry of the Arctic Ocean; *in* Arctic Geophysical Review, edited by J.F. Sweeney, Department of Energy, Mines and Resources, v. 45, p. 7-14.

Sobczak, L.W. and Weber, J.R.
1986: Gravity and bathymetry along seismic refraction lines, Canadian Ice Island, N.W.T., April 18-May 2, 1986; Geological Survey of Canada, Geophysics Division, Internal Report No. 86-13, Ice Island Contribution No. 5, p. 1-14.
1987: Gravity and bathymetry taken along seismic refraction lines from the Canadian Ice Island during 1985 and 1986; *in* Current Research, Part A, Geological Survey of Canada, Paper 87-1A, p. 299-304.

Sobczak, L.W., Hearty, D.B., Forsberg, R., Kristoffersen, Y., Eldholm, O., and May, S.D.
1990: Gravity of the Arctic Ocean; *in* The Arctic Region, edited by A. Grantz, L. Johnson, and J.F. Sweeney, Geological Society of America, The Geology of North America, v. L, Plate 3.

Sobczak, L.W., Mayr, U., and Sweeney, J.F.
1986: Crustal section across the Polar continent-ocean transition in Canada from Somerset Island to the Canada Basin; Canadian Journal of Earth Sciences, v. 23, p. 608-621.

Sobczak, L.W., Weber, J.R., and Roots, E.F.
1970: Rock densities in the Queen Elizabeth Islands, Northwest Territories; Proceedings of the Geological Association of Canada, v. 21, p. 5-14.

Sweeney, J.F., Mayr, U., Sobczak, L.W., and Balkwill, H.R.
in press: The Polar continent-ocean transition in Canada (Corridor G); *in* Phanerozoic Evolution of North American Continent-Ocean Transitions, edited by R.C. Speed, Geological Society of America, Centennial Continent/Ocean Transect Volume CTV-1, Contribution from the Earth Physics Branch No. 1175.

Thorsteinsson, R. and Trettin, H.P.
1971a: Cape Stallworthy, District of Franklin; Geological Survey of Canada, Map 1305A.
1971b: Otto Fiord, District of Franklin; Geological Survey of Canada, Map 1309A.
1971c: Bukken Fiord, District of Franklin; Geological Survey of Canada, Map 1310A.
1971d: Greely Fiord, District of Franklin; Geological Survey of Canada, Map 1311A.

Trettin, H.P. and Parrish, R.
1987: Late Cretaceous bimodal magmatism, northern Ellesmere Island: isotopic age and origin; Canadian Journal of Earth Sciences, v. 24, p. 257-265.

Weber, J.R.
1986: The Alpha Ridge: gravity, seismic and magnetic evidence for a homogeneous, mafic crust; Journal of Geodynamics, v. 6, p. 117-136.

Weber, J.R. and Cooper, R.V.
1988: Crustal structure of the Alpha Ridge and eastern Canada Basin; Abstract, Joint Annual Meeting, Geological Association of Canada, Mineralogical Association of Canada and Canadian Society of Petroleum Geology, St. John's, Newfoundland, v. 13, p. A133.

Weber, J.R. and Sobczak, L.W.
1986: Arctic Ocean bathymetry using the seismic sounding method; Geological Survey of Canada, Ice Island Contribution No. 4, Geophysics Division, Internal Report No. 86-13, p. 1-8.

Worzel, J.
1968: Advances in marine geophysical research of continental margins; Canadian Journal of Earth Sciences, v. 5, p. 458-469.